Department of Urology, University Hospital of Ulm

Acting Medical Director: PD Dr. med. Florian Jentzmik

Functional relevance of the candidate genes *MSMB, NCOA4, TIMM23* and *PARG* in the prostate cancer risk region 10q11 for the emergence of oncogenic *TMPRSS2:ERG* fusions

DISSERTATION

for the degree

Doctor of Medicine (Dr. med.)

Faculty of Medicine, Ulm University

submitted by

Andrea Nottelmann Mariné

born in Barcelona, Spain

2014

Current Dean: Prof. Dr. rer. nat. Thomas Wirth

1. Supervisor: PD Dr. hum. biol. Christiane Maier

2. Supervisor: Prof. Dr. Günter Assum

Day of Thesis Defense: November 20th, 2015

Table of Contents

List of Abbreviations..... III

1. Introduction.....1

1.1. Prostate cancer..... 1

1.1.1. Risk factors..... 1

1.1.2. Prostate Cancer Genome-Wide Association Studies 2

1.2. The prostate cancer variant rs10993994 in the risk locus 10q11 2

1.2.1. Candidate genes in 10q11 3

1.2.2. Mechanisms driving prostate cancer risk in 10q11..... 4

1.3. Rationale..... 6

2. Materials and Methods.....8

2.1. Materials..... 8

2.1.1. Chemicals..... 8

2.1.2. Solutions, buffers and culture media 8

2.1.3. Reagent Kits..... 9

2.1.4. Cell lines..... 9

2.1.5. Laboratory Equipment..... 9

2.1.6. Plastic and Glassware 10

2.1.7. Oligonucleotides and quantitative RT-PCR probes 10

2.1.8. Small interfering RNAs (siRNAs) 10

2.2. Methods 12

2.2.1. Cell culture procedures 12

2.2.2. SiRNA transfection..... 13

2.2.3. RNA isolation 14

2.2.4. Polymerase chain reaction (PCR) and related methods..... 14

2.2.5. *TMPRSS2:ERG* induction assay 19

2.2.6. MTT-viability test..... 21

2.2.7. Statistical analysis..... 21

3. Results.....22

3.1. Influence of down-regulation of *MSMB, NCOA4, TIMM23* and *PARG* on the generation of *TMPRSS2:ERG* fusions..... 22

3.1.1. Time response curves of target gene expression after siRNA transfection 22

3.1.2. Dose-dependent effects of γ-radiation on *TMPRSS2:ERG* fusion induction and *TMPRSS2* expression 23

3.1.3. Quantification of *de novo TMPRSS2:ERG* fusions after down-regulation of *MSMB*, *NCOA4*, *TIMM23* and *PARG* 25

3.2. Influence of down-regulation of *PARP1* on the generation of *TMPRSS2:ERG* fusions 27

3.2.1. Establishing PARP1 mRNA quantification 27

3.2.2. Quantification of *de novo TMPRSS2:ERG* fusions at standard siPARP1 knock-down 28

3.2.3. Toxicity of siPARP1 treatment on LNCaP cells 29

3.2.4. Quantification of *de novo TMPRSS2:ERG* fusions at modified siPARP1 knock-down 32

4. Discussion 34

4.1. Functional relevance of *MSMB*, *NCOA4*, *TIMM23* and *PARG* for the generation of *TMPRSS2:ERG* fusions in prostate cancer 34

4.2. Functional relevance of *PARP1* and the poly(ADP-ribose) level for the generation of *TMPRSS2:ERG* fusions in prostate cancer 40

4.3. Advantages and limitations of the *TMPRSS2:ERG* induction assay 41

4.4. DNA repair and its implication in prostate cancer pathogenesis and in the generation of *TMPRSS2:ERG* fusions 42

4.5. Clinical relevance of *TMPRSS2:ERG* fusions in prostate cancer 43

4.6. Conclusions 44

5. Summary 46

6. Literature 47

Acknowledgements 58

Curriculum vitae 59

List of Abbreviations

A	adenine
ABL	Abelson Murine Leukemia Viral Oncogene Homolog 1
ADP	adenine-dinuclotide-phosphate
AR	androgen receptor
ATM	ataxia teleangiectasia mutated protein
BCR	breakpoint cluster region
bp	base pairs
C	cytosine
cAMP	cyclic adenine-mononucleotide phosphate
cDNA	complementary desoxyribonucleic acid
CI	confidence interval
CML	chronic myeloid leukemia
CO_2	carbon dioxide
CREB	cAMP response element binding protein
C_t	cycle threshold
DHT	dihydrotestosterone
DNA	desoxyribonucleic acid
dsRNA	double strand ribonucleic acid
ETS	E-twenty-six
FLI	Friend leukemia integration transcription factor
FRET	fluorescence resonance energy transfer
G	guanine
GWAS	genome-wide association studies
Gy	Gray
h	hours
h^2	heritability
HGPIN	high-grade prostatic intraepithelial neoplasia
HR	homologous recombination
IR	irradiation
M	molar
MAF	minor allele frequency
MGB	minor groove binder
MMP	matrix metalloproteinase
mRNA	messenger ribonucleic acid
n	number of experiments
NADPH	nicotinamide adenine dinucleotide phosphate
NAD^+	nicotinamid adenine dinucleotide
NHEJ	non-homologous end joining
OR	odds ratio
PCR	polymerase chain reaction
PIN	prostate intraepithelial neoplasia
PR	progesterone receptor
PSA	prostate specific antigen

pTNM	TNM Classification of Malignant Tumors
Q	relative expression of target gene
qPCR	quantitative polymerase chain reaction
R^2	coefficient of determination
ref	reference sample
RISC	RNA-induced silencing complex
RNA	ribonucleic acid
RNAi	RNA interference
rpm	rounds per minute
RR	relative risk
RT	reverse transcription
SEM	standard error of the mean
siRNA	small interfering ribonucleic acid
SNP	single nucleotide polymorphism
SOI	sample of interest
T	thymine
VDR	vitamin D receptor
VEGF	vascular endothelial growth factor

1. Introduction

1.1. Prostate cancer

1.1.1. Risk factors

Prostate cancer is the second most frequently diagnosed cancer among men in developed countries and the fourth most common cancer overall [25]. Age-standardized incidence rates are high in Australia/New Zealand, Northern America, Northern and Western Europe (~80-112 per 100.000 depending on the country), intermediate in the Caribbean and Southern Africa (80 and 62 per 100.000 respectively) and low in Eastern and South-Central Asia (11 and 5 per 100.000 respectively) [25]. Use of prostate-specific antigen (PSA) for early detection screening programs in some countries contributes to the gradient of incidences. Established risk factors for prostate cancer are an advanced age, ethnicity and a positive family history [7, 35]. Environmental and lifestyle-related factors may also play a role [48, 59]. According to meta-analyses of family studies the relative risk (RR) for men with an affected first-degree relative is 2.22-fold higher than for those with a negative family history (95% confidence interval (CI) 2.06 - 2.4) [7]. Furthermore, twin studies identified prostate cancer as the tumor with the highest heritability among all frequent tumors ($h^2 = 0.42$, 95% CI 0.29 - 0.5) [48]. Despite this strong evidence for genetically determined disease risk, the search for prostate cancer susceptibility genes is still unsatisfying. To date, predisposing germ line mutations in the genes *HOXB13* and *BRCA2* have been identified. Nevertheless, they only account for a small percentage of prostate cancer cases [19, 23]. *HOXB13* encodes a highly conserved homeobox transcription factor of the HOX superfamily, which is important for the development of the urogenital system in vertebrates [100]. Recent studies identified that the *HOXB13* mutation was present in ~5 % of prostate cancer families and that it was significantly higher in patients with early-onset familial cancer than in those with late-onset, non-familial cancer (3.1 % compared to 0.6% respectively) [23, 97]. The *BRCA2* gene, already known for its causal role in hereditary breast cancer, is a tumor suppressor gene involved in the homologous recombination of the DNA repair machinery. Two percent of men with early-onset prostate cancer harbor a germ line mutation in the *BRCA2* gene [19]. They have a 23-fold higher risk of developing cancer than non-carriers. These findings suggest

that prostate cancer may follow a polygenetic inheritance with a potential involvement of further high-risk susceptibility genes that have not been identified so far.

1.1.2. Prostate Cancer Genome-Wide Association Studies

Genome-wide association studies (GWAS) have successfully identified inherited genetic variants that influence disease risk. In a case-control configuration, GWAS are designed to identify common low to moderate risk-associated variants that occur at a minor allele frequency (MAF) greater than 5% [38]. Other risk-modulating influences such as rare variants, epigenetic changes or structural rearrangements in the DNA structure cannot be assessed by GWAS. Prostate cancer GWAS have so far identified over 70 risk-associated variants accounting for 30% of the inherited risk for disease [21]. Each of these variants contributes to the overall susceptibility with a small additive effect (typically with per-allele odds ratio (OR) less than 2) [31]. In terms of a multifactorial inheritance, enrichment of multiple risk alleles in one individual patient can have substantial cumulative effects [84, 101]. This seems to have a promising use in genetic risk prediction and early screening programs [52]. However, for the majority of risk alleles, the underlying functional mechanisms of disease susceptibility remain elusive. A great majority of variants lie in intronic or intergenic regions, such as 3p12, 8q24 or 11q13 [39], making it challenging to understand how the variants interact with gene expression or with downstream signaling pathways. The risk loci 10q11, as described below in more detail, is a region in which the causative gene for the observed risk increase is not yet identified among several potential candidates.

1.2. The prostate cancer variant rs10993994 in the risk locus 10q11

Extensive data from a comprehensive set of genome-wide association studies identified the polymorphism rs10993994 as prostate cancer risk variant [21, 41, 85]. The variant lies on the long arm of chromosome 10, 2 base pairs (bp) upstream of the transcription origin of the microseminoprotein beta gene (*MSMB*) [42]. Direct neighbors are the genes nuclear receptor coactivator 4 (*NCOA4*), translocase of the inner mitochondrial membrane 23 (*TIMM23*) and poly(ADP-ribose) glycohydrolase (*PARG*) as well as two partial genomic duplications of *PARG* and *TIMM23* (*PARGP1* and *TIMM23B*). **Figure 1**

gives an exemplary overview of the 10q11 locus based on data from the USCS Genome Browser of Human (http://genome-euro.ucsc.edu/; human reference sequence GRCh37).

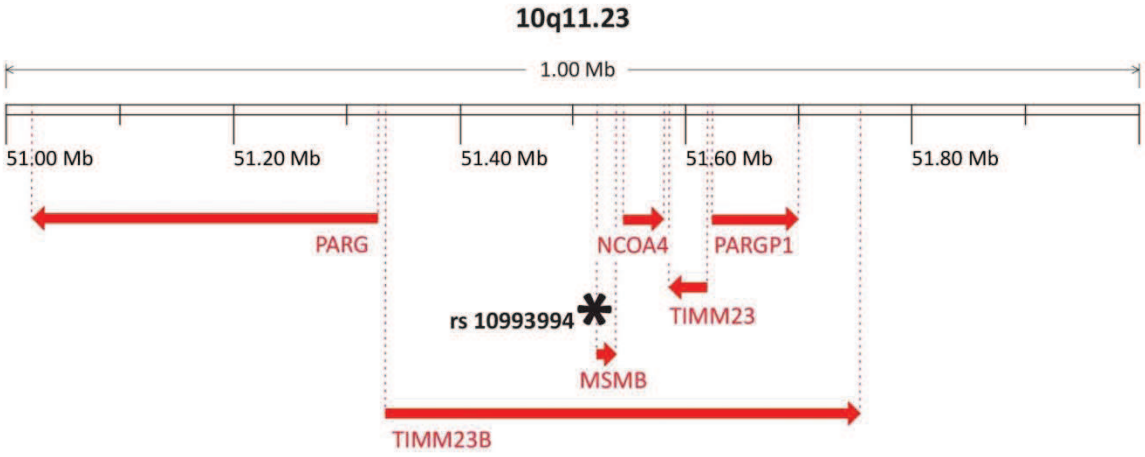

Figure 1: Schematic overview of the locus 10q11. The single nucleotide polymorphism rs10993994 lies in the promoter region of the *MSMB* gene on the long arm of chromosome 10 and is marked by a black asterisk. The genes *NCOA4*, *TIMM23* and *PARG* as well as the partial genomic duplications of *PARG (PARGP1*) and *TIMM23 (TIMM23B*) are located in the direct surrounding. Gene symbols are given in their short form abbreviation and are marked by red arrows. Abbreviations: Mb = megabase, rs = reference single nucleotide polymorphism identification number.

1.2.1. Candidate genes in 10q11

Microseminoprotein beta (*MSMB*)

Microseminoprotein beta (*MSMB*) encodes the prostate secretory protein of 94 amino acids (PSP_{94}), one of the major components of the seminal fluid [50]. The *MSMB* gene was the first to be investigated as candidate gene for the prostate cancer risk variant rs10993994. *In-vitro* luciferase reporter assays demonstrated that the risk allele of the variant reduces the *MSMB* promoter activity by alteration of a transcription factor binding site [11, 56]. *MSMB* expression was found down-regulated in tumorigenic prostatic tissue on both mRNA and protein level [10, 67, 81]. Thus, *MSMB* has long been an unquestioned tumor suppressor gene in the pathogenesis of prostate cancer.

Nuclear receptor coactivator 4 (*NCOA4*)

NCOA4 encodes the androgen receptor associated protein 70 (ARA_{70}), a co-activator of different nuclear receptors such as the androgen receptor (AR) [98], the progesterone receptor (PR) [98] and the vitamin-D receptor (VDR) [86]. In the presence of

dihydrotestosteron (DHT) and testosterone, ARA_{70} binds to the AR and enhances the transcriptional activity of androgen dependent genes [98].

Translocase of the inner mitochondrial membrane 23 (*TIMM23*)

The gene for the translocase of the inner mitochondrial membrane 23 (*TIMM23* also known as *TIM23*) encodes a protein of the channel-forming unit of the Tim23 complex, a multicomponent translocase, which enables the passage of mitochondrial proteins from the cytosol into the mitochondrial matrix [58]. Cells induced to undergo apoptosis in the presence of caspase inhibitors seem to selectively degrade Tim23 causing cell death [30].

Poly(ADP-ribose) glycohydrolase (*PARG*)

With its main counterpart the poly(ADP-ribose) polymerase 1 (*PARP1*), *PARG* tightly regulates a great number of cellular processes such as DNA replication and DNA repair, post-translational modification of proteins and apoptosis [16]. *PARP1* transfers ADP-ribose from nicotinamide adenine dinucleotide (NAD^+) on a variety of target proteins generating large protein-bound poly(ADP-ribose) polymers. To revert this reaction *PARG* cleaves poly(ADP-ribose) ends and degrades the polymers [16]. Protein-free poly(ADP-ribose) polymers are signaling molecules inducing cell death [3].

1.2.2. Mechanisms driving prostate cancer risk in 10q11

Multiple genome-wide association studies have identified the SNP rs10993994 in 10q11 as prostate cancer risk variant [21, 41, 85]. Since the variant lies in a non-coding region, the underlying biological mechanisms of disease susceptibility are not clear to date. However, the findings of several functional studies have suggested that the variant is associated with alterations in the gene expression of local genes, with impairments in the cellular DNA repair capacity and with the generation of oncogenic chromosomal rearrangements.

Genes transcriptionally altered by the variant rs10993994

The risk allele of the prostate cancer variant rs10993994 has shown to potentially influence multiple neighboring candidate genes in their expression. First *in-vitro* reporter assays proved that the risk allele of the variant reduces the *MSMB* promoter activity by disrupting the cAMP response element-binding protein (CREB) binding site [11, 56]. In

search for other putative candidate genes, Pomerantz *et al.* investigated the genotype-dependent expression of *MSMB*, *NCOA4* and *TIMM23* in prostatic tissue. They found that the risk allele of the variant was associated with a down-regulated *MSMB* expression in histologically normal and malignant prostatic tissue as well as with an increased expression of *NCOA4* in normal prostatic tissue. The expression level of *TIMM23* seemed not to be correlated with the genotype status in either normal or tumor tissue [74]. Recent investigations about the expressional status of more candidate genes in 10q11 were able to reproduce the described findings for *MSMB* [78]. Furthermore, the risk genotype of the variant was significantly associated with *NCOA4* overexpression in tumor tissue. *TIMM23B* expression (the partial duplication of *TIMM23*) also correlated significantly with the number of risk alleles in histologically normal prostatic tissue [78]. Considering these associations, germline variation at 10q11 may contribute to elevated prostate cancer risk by influencing more than one candidate gene.

Association between the variant rs10993994 and impairments in the cellular DNA repair capacity

In order to correlate known prostate cancer risk loci with established features of malignancy, Rinckleb *et al.* investigated a panel of 14 known prostate cancer risk SNPs for their influence on the DNA repair capacity [79]. Blood lymphocytes of healthy donors were genotyped and analyzed for their response to DNA damage. Among the series tested, the risk associated variant rs10993994 showed an association with impaired DNA double strand break repair [79].

Association between the variant rs10993994 and the oncogenic *TMPRSS2:ERG* rearrangement

Somatic gene fusions are found in a variety of cancers: the *BCR-ABL* translocation [t(9;22)] in chronic myeloid leukemia (CML), the *ETS-FLI* translocation [t(11;22)] in Ewing sarcoma and further rearrangements involving *ETS* family members in prostate cancer. Most commonly, *ERG*, an *ETS* gene, becomes fused to *TMPRSS2*, a serine protease of yet unknown function [88]. The fusion event places the *ERG* proto-oncogene under the control of the androgen-regulated promoter of *TMPRSS2*, enhancing its expression [88]. *ERG* overexpression is believed to cause alterations in several pathways such as stem cell development, cell senescence, proliferation, migration and apoptosis [12]. Found in ~50%

of prostate cancer cases, the *TMPRSS2:ERG* fusion is likely to be the most common rearrangement found in human malignancies [72, 88, 89]. Several studies with *in-vitro* and *in-vivo* model systems have concluded that the *TMPRSS2:ERG* fusion occurs early in the tumor development and mediates the transition from prostate intraepithelial neoplasia (PIN) to frank prostate cancer [72, 87]. The *ETS* fusion positive prostate cancer is probably a tumor entity distinct from *ETS* fusion negative prostate cancers and has features of its own molecular pattern [65, 76].

Attempting to identify the mechanistic relevance of verified prostate cancer variants, Rinckleb *et al.* tested a panel of 27 risk SNPs for a correlation with the somatic *TMPRSS2:ERG* fusion status. Four of the 27 SNPs tested were associated with a positive *TMPRSS2:ERG* fusion status, including the variant rs10993994 [78]. As gene fusions may result from an error-prone DNA repair after DNA double-strand breaks, 10q11 might be associated with the *TMPRSS2:ERG* fusion due to its involvement in DNA repair.

1.3. Rationale

Common germline variants play a substantial role in the overall strong heritability of prostate cancer. While integration of the predictive value of a series of risk variants is considered in different screening settings for early tumor detection, functional knowledge for the majority of known loci is lagging behind. At 10q11, the non-coding SNP rs10993994 is associated with prostate cancer risk and its genotype variation potentially influences multiple surrounding candidate genes in their expression. Previous work has suggested that the rs10993994 is correlated with two classical features of carcinogenesis, namely altered DNA repair and higher incidences of the oncogenic chromosomal rearrangement between *TMPRSS2* and *ERG*. The present work is based on the pathomechanistic hypothesis, that this locus mediates prostate cancer risk via error-prone double strand break repair, hence promoting oncogenic rearrangements. The study aim was to investigate the candidate genes *MSMB*, *NCOA4*, *TIMM23* and *PARG* for their functional involvement in the *TMPRSS2:ERG* formation in order to identify the causal gene for the observed association between the rs10993994 and the presumed prostate cancer risk pathomechanism. In addition, the *PARP1* gene, which is not located within the chromosomal region of interest, was also tested on its effect on the formation of fusions.

PARP1 represents an important mediator of DNA damage repair and is the functional opponent of *PARG.*

In the present work, each candidate's gene expression was down-regulated through siRNA in order evaluate its effect on the generation of *TMPRSS2:ERG* fusions. By applying the *TMPRSS2:ERG* induction assay, androgen-responsive prostate cancer cells were prompted to generate *de novo TMPRSS2:ERG* fusions and to express quantifiable fusion transcripts. In an established procedure, cells were treated with a combination of dihydrotestosterone (DHT) and γ-radiation. To assure a strong down-regulation at the time of fusion induction, time-response curves for all gene expressions after siRNA transfection were generated. The relative expression levels were quantified 24 h, 48 h, 72 h, 96 h and 120 h after transfection by quantitative Real Time PCR (qRT-PCR). The time of fusion induction was chosen according to the time-point of best knock-down efficacy for all gene expressions. To obtain a strong fusion induction, different γ-radiation doses were tested on their potential to generate *TMPRSS2:ERG* fusions. Once the optimal protocol was established, each gene was separately down-regulated in LNCaP cells and fusions were generated. As outcome of the gene fusion induction assay, *TMPRSS2:ERG* transcripts were quantified by qRT-PCR.

2. Materials and Methods

2.1. Materials

2.1.1. Chemicals

2-Mercapthoethanol (MEtOH)	Sigma-Aldrich, München, Germany
Acetic acid (AcOH)	Merck, Darmstadt, Germany
Dihydrotestosterone (DHT)	Sigma-Aldrich, München, Germany
Dimethylsulfoxide (DMSO)	Sigma-Aldrich, München, Germany
Ethanol 70% (EtOH)	Honeywell, Germany
Ethylenediaminetetraacetic acid (EDTA)	Fluka, Neu-Ulm, Germany
Fetal calf serum (FCS)	Biowest, Nuaillé, France
Fetal calf serum, hormone reduced (FCS dcc)	Biowest, Nuaillé, France
Hydrochloric acid (HCl), 1M	Merck, Darmstadt, Germany
MTT (3-*(4,5-dimethylthiazol-2-yl)-2,5-diphenyl-tetrazoliumbromide*)	Sigma-Aldrich, München, Germany
Sodium dodecyl sulfate (SDS)	Sigma-Aldrich, München, Germany
Tris(hydroxylmethyl)aminomethane (TRIS)	Sigma-Aldrich, München, Germany
Trypsin	PAA Laboratories GmbH, Pasching, Austria

2.1.2. Solutions, buffers and culture media

MTT-dye

MTT (3-*(4,5-dimethylthiazol-2-yl)-2,5-diphenyl-tetrazoliumbromide*)
in phospate buffered saline (PBS) (5 mg/ml)

MTT lysis buffer (pro ml)

DMSO 994µl
SDS 100mg
Acetic acid 6µl

Opti-MEM I gibco® transfection medium	Invitrogen, Life Technologies, Carlsbad, USA
PBS buffer(without Ca^{2+} & Mg^{2+})	PAA Laboratories GmbH, Pasching,

	Austria
Penicillin-Streptomycin Solution (100x)	PAA Laboratories GmbH, Pasching, Austria
RPMI 1640 medium	PAA Laboratories GmbH, Pasching, Austria
TE buffer for TaqMan® probe dilution TRIS 1mM EDTA 10 µM in RNase-free H_2O, pH 8.0 (HCl)	
Trypsin (0.05%) - EDTA (0.02%) in PBS	PAA Laboratories GmbH, Pasching, Austria

2.1.3. Reagent Kits

Lipofectamine® RNAiMAX Reagent	Invitrogen, Life Technologies, Carlsbad, USA
QIAShredder	Qiagen, Hilden, Germany
QuantiFast Multiplex RT-PCR + R Kit	Qiagen, Hilden, Germany
RNase free DNase Set	Qiagen, Hilden, Germany
RNeasy Mini Kit	Qiagen, Hilden, Germany

2.1.4. Cell lines

The human prostate cancer cell line LNCaP, which originated from a lymph node metastasis, was purchased from the American Type Culture Collection (ATCC), Manassas, USA.

2.1.5. Laboratory Equipment

Cell counter Model 2000	AL-Systeme, Karlsruhe, Germany
Centrifuge 5417R	Eppendorf, Hamburg, Germany
Centrifuge Megafuge 1.OR	Heraeus Instruments, Osterode, Germany
Centrifuge Megafuge 40R	Thermo Scientific, Langenselbold,

	Germany
Incubator Hera cell 240 37°C + 5% CO_2	Thermo Scientific, Langenselbold, Germany
Gammacell 2000, Cs-137 source, 3.3Gy/min	Molsgaard Medical, Heorsholm, Denmark
SLT Spectra photometer	SLT Labinstruments, Crailsheim, Germany
ViiA™ 7 Real-Time PCR-System	Applied Biosystems, Life Technologies, Carlsbad, USA

2.1.6. Plastic and Glassware

MicroAmp® Fast Optical 96-Well Reaction Plate	Applied Biosystems, Life Technologies, Carlsbad, USA
MicroAmp® Adhesive Film	Applied Biosystems, Life Technologies, Carlsbad, USA
Pipet tips and reagent tubes	Sarstedt, Nümbrecht, Germany

2.1.7. Oligonucleotides and quantitative RT-PCR probes

Unlabeled Primers were purchased from biomers.net (Ulm, Germany). The TaqMan® probes for the TaqMan® detection assays were obtained from Applied Biosystems, Life Technology (Carlsbad, USA). For the expression analysis of the *PARP1* gene a pre-designed gene expression assay from Applied Biosystems, Life Technologies (Carlsbad, USA) was used (Assay ID: Hs00242302_m1). All specific primer sequences and TaqMan® probe sequences are given in **Table 1**.

2.1.8. Small interfering RNAs (siRNAs)

Gene specific siRNAs were obtained from Qiagen (Hilden, Germany). The particular sequences of the commercially available mixture of pre-designed siRNAs are given in **Table 2**. The non-specific mixture of the AllStars Negative Control siRNA was purchased from the same company.

Table 1: Sequences of gene-specific primers and Taqman® probes used for real-time PCR (5 '- 3'). Target genes are given in their short form abbreviation and are printed in bold type. The specific sequences for primers and probes are listed below. The respective dye for each Taqman® probe is specified in parentheses. Abbreviations: A = adenine, C = cytosine, FAM = TaqMan® FAM™ dye, G = guanine, T = thymine, VIC = TaqMan® VIC® dye.

TARGET	SEQUENCES
G6PD	
forward primer	CCGGGCATGTTCTTCAA
reverse primer	AGGGAGCTTCACGTTCTTGTAT
probe (VIC)	TCCAGCTCCGACTCC
MSMB	
forward primer	CTGTCTATAAGGAGTCCTGCTTATCA
reverse primer	TGCATTGCATAAAGTCACGA
probe (FAM)	ATCTTTGCCACCTTCGT
NCOA4	
forward primer	CAGCAGCTCTACTCGTTATTGG
reverse primer	TCTCCAGGCACACAGAGACT
probe (FAM)	TCAATTGTCTTACTCATCAAC
TIMM23	
forward primer	ATTTGGTGTCATCATTGAGAAAAC
reverse primer	TGCTATCCCTCGAAGACCA
probe (FAM)	ATGACCTTAACACAGTAGCA
PARG	
forward primer	GCACTGAGATCGTTGCCAT
reverse primer	AGAAATCCACAGTAAGCCTTGTT
probe (FAM)	CTTCACTTCAGACGCTAC
TMPRSS2	
forward primer	CAGGGACATGGGCTATAAGAA
reverse primer	AGTTTCATAAAGCTGGTGGATC
probe (FAM)	CTATTCCTTGGCTAGAGTAA
T1G4	
forward primer	TGGAGCGCGGCAGGAAG
reverse primer	TCCGTAGGCACACTCAAACA
probe (FAM)	TCCTCACTCACAACTGATAA
ESCO1	
forward primer	ATTTGGCCAATGAGATAAAACCT
reverse primer	CAAACATTGGCTGAAATTCTTAT
probe (FAM)	ATGCTGAATCAAAAGAATGT

Table 2: Sequences of small interfering RNAs (siRNAs). Target genes are given in their short form abbreviation and are printed in bold type. The specific siRNAs with their corresponding product names and sequences are listed below. Abbreviations: A = adenine, C = cytosine, G = guanine, LOC = locus identification, T = thymine.

siRNA	SEQUENCES
MSMB	
MSMB_5	AAGACCTGTTCTGTCAGTGAA
MSMB_7	ACACCTGTGGGTTATGACAAA
MSMB_8	AGGGAGTTCCAGGAGATTCAA
MSMB_9	ATGCTATTTCATACCTAATGA
NCOA4	
NCOA4_1	CTGGTCAATAGTGATTACCA
NCOA4_3	CCCACGTTAGTTCTACATTAT
NCOA4_4	AAGAGAAGTGGTTATATCGAA
NCOA4_5	ACCGACTAAGCAAATAGGCAA
TIMM23 (LOC1002)	
LOC1002_1	TACCAGCCTCTCTGCACTATA
LOC1002_2	ACAGGTGGTCTTCGAGGGATA
LOC1002_3	AACCATGACAGGCATGTTGTA
LOC1002_4	ATCACCAAGTCCATTCATTTA
PARG	
PARG_2	CTGGATCACAATGAATGTCTA
PARG_5	TTGCTACGATACTACAATGAA
PARG_6	AACAGTAACCCTGGTACCAGA
PARG_7	AAGGGCGGTGAAGTTAGATTA
PARP1	
PARP1_5	CATGGGCTATAAGAA
PARP1_6	ACGGTGATCGGTAGCAACAAA
PARP1_7	AAGGCGAATGCCAGCGTTACA
PARP1_8	TCCCATCGATGTCAACTATGA
ESCO1	
ESCO1_5	AACCGGAGATCACAAAGGCTA
ESCO1_6	CTCGCATGATTGAATGCCTAA
ESCO1_7	CAAGTGAATCGAAGTCCAATA
ESCO1_8	CAAGAAGGTCGTTACGCAGTA

2.2. Methods

2.2.1. Cell culture procedures

A human prostate cancer cell line originated from lymph node metastasis (LNCaP) was grown in RPMI 1640 culture medium (containing 15% fetal calf serum (FCS) and 1% penicillin/streptomycin) and maintained in a humid atmosphere at 37°C and 5% CO_2. To guarantee defined hormone levels in all *TMPRSS2:ERG*-related procedures, including

seeding and transfection, RPMI 1640 with hormone-reduced fetal calf serum stripped with dextran-coated charcoal (FCS dcc) was used. Routine seeding procedures were performed as follows. Cells were washed with 5 ml PBS buffer. 3 ml trypsin-EDTA solution were added to detach the cells from the bottom surface. After a 5-minute incubation period, the trypsin treatment was stopped by adding 7 ml of RPMI 1640 medium. Subsequently, cells were centrifuged at 1000 rounds per minute (rpm) for 5 minutes, the supernatant was discarded and the cells resuspended in 2 ml medium. Aliquots of 50 µl were taken to determine the number of cells for the following experiments using a cell counter.

2.2.2. SiRNA transfection

Small interfering RNAs (siRNAs) are 20 to 25 base pairs (bp) long, double-stranded RNA molecules (dsRNA). SiRNAs are delivered into living cells by lipid-based transfection reagents silencing specific genes by RNA interference (RNAi). The guide strand of the dsRNA is recognized and incorporated into the RNA-induced silencing complex (RISC) directing the complex to the complementary messenger RNA (mRNA). Multiple nucleases within the complex cleave and degrade the target mRNA impeding its translation.

In the present work, gene silencing was used to analyze the relevance of candidate genes for the formation of *TMPRSS2:ERG* fusions. LNCaP cells were transfected with siRNA using Lipofectamine® RNAiMAX Reagent. To reduce unspecific, off-target effects a mixture of four different siRNAs per gene was used. A reverse transfection protocol was performed where the addition of cells and siRNA was done in reverse order. This yielded better results than using the conventional procedures. For each targeted gene, four siRNAs (each 25 nM) were prepared on ice. 960 µl of Opti-MEM-I medium and 10 µl of Lipofectamine® RNAiMAX Reagent were added. Incubation at room temperature for 15 to 20 minutes induced the formation of transfection complexes. LNCaP cells were harvested and diluted in hormone-reduced RPMI 1640 medium to obtain 300.000 cells per ml. Transfection complexes were given into a cell culture flask (25 cm^2) and 5 ml of cell suspension were added on top. The final siRNA concentration was 20 µM.

2.2.3. RNA isolation

RNA from cells were isolated using the RNeasy Mini Kit from Qiagen (Hilden, Germany). For cell lysis, RLT buffer was previously mixed with 1% of mercaptoethanol and directly given to the adherent cells. The cell suspension was loaded on QiaShredder (Qiagen®, Hilden, Germany) homogenizers that consist of a biopolymer-shredding membrane in a microcentrifuge spin-column. After 2 minutes of centrifugation at 14000 rpm, the flow-through was mixed with one volume of 70% ethanol and transferred to silica membrane spin columns. Residual ethanol was removed with 350 µl of RW1 buffer. An on-column DNAse treatment using an RNAse-free DNAse set (Qiagen®, Hilden Germany) was performed in the course of the RNA isolation procedure. According to the manufacturer's instructions, multiple washing steps with two buffers (RW1 and RPE) were performed in order to clean the RNA from remaining contaminants. Finally, the RNA was eluted in 30 µl of RNAse-free water and stored at -70°C.

2.2.4. Polymerase chain reaction (PCR) and related methods

Classic PCR

The polymerase chain reaction (PCR) is the most powerful amplification technique of linear DNA. It is based on a cycle of three steps - denaturation, primer annealing and elongation. These steps are carried out in a thermal cycler that sequentially allows rapid temperature changes and cycle repetitions. The product of one cycle is the starting product for the next one leading to an exponential increase in DNA concentration. For the denaturation of the DNA double strands hydrogen bonds between complementary nucleotides are destroyed. This requires temperatures of 94°C to 98°C. Once the DNA strands have separated, primers can anneal. These small oligonucleotides are complementary to the flanking ends of the sense and antisense target DNA, respectively. They have a free 3'-hydroxy group to allow addition of further nucleotides via phosphodiester bonds. Thus, a heat-stable DNA polymerase is recruited and begins to add complementary nucleotides to the elongating strand. After that, DNA double strands are separated again by thermal denaturation and a new cycle of replication begins.

Quantitative Real Time PCR (qRT-PCR)

A classic PCR can be modified in order to quantify gene expression by generating and

amplifying DNA copies of the respective mRNA. This is done in the quantitative Real Time PCR. Transcription of RNA in copy DNA (cDNA) is a prior step combined with subsequent quantitative PCR (qPCR). Amplification of a specific sequence in the DNA, its detection and quantification is all performed in parallel.

In this work the OneStep RT-PCR Kit from Qiagen® (Hilden, Germany) and the ViiA™ 7 Real-Time PCR System purchased by Applied Biosystems, Life Technologies (Carlsbad, USA) were used (Software version v1.2).

The expression level of target genes was measured relative to the mRNA of a reference gene with the $\Delta\Delta C_t$ method. This approach is more robust to deviations than an absolute quantification.

First-strand cDNA synthesis

During cDNA transcription mixtures of primers with arbitrary sequences of 6 bp in length, so called random hexamers, bind non-specifically to the RNA. This random priming allows transcription of the entire RNA into cDNA by the reverse transcriptase (RT). For optimal primer annealing and nucleotide polymerization, this step is performed at 50°C.

qPCR

Quantitative expression analyses were performed by monitoring the fluorescence intensity of TaqMan® probes for every cycle (‘real time’) in a gene specific PCR. TaqMan® probes are DNA probes with a specific fluorophore at the 5´-end and a quencher at the 3’-end. Tagged to the quencher is a minor groove binder (MGB), which increases the probe’s melting temperature and stabilizes the probe-template interaction. Before elongation of the DNA strand, the annealed probe stays intact allowing the quencher to suppress fluorescence intensity of the fluorophore via fluorescence resonance energy transfer (FRET). When the DNA polymerase elongates the leading strand, probes are degraded by the enzyme’s 5’-3’-exonuclease activity and the fluorophore and the quencher are spatially separated. Fluorescence can now be detected by the real-time PCR system. The reaction set-up and the qRT-PCR program are listed in **Table 3** and **Table 4**.

Table 3: Exemplary reaction set-up for a singleplex quantitative real-time PCR. Abbreviations: c = concentration, *TIMM23* = gene symbol for the translocase of the inner mitochondrial membrane 23, ∑ = total, µl = microliter, µM = micromolar.

Component	Volume (µl) per well
2x Quantifast Multiplex RT-PCR Master Mix + ROX	10.4
Forward primer final concentration of 0.1 µM, except for *TIMM23* (c=0.05 µM)	0.2
Reverse primer final concentration of 0.1 µM, except for *TIMM23* (c=0.05 µM)	0.2
TaqMan probe	0.2
Quantifast Multiplex RT Mix	0.2
Template RNA	1.0
RNAse free water	7.8
	∑ 20.0

Table 4: Cycling program for the quantitative real-time PCR using QuantiFast Multiplex RT-PCR + R Kit. Abbreviations: min = minutes, sec = seconds, *TMPRSS2:ERG* = gene symbol for the rearrangement between the genes *TMPRSS2* and *ERG,* °C = degrees Celsius.

Step	Time	Temperature	Cycles
reverse transcription & cDNA generation	20 min	50°C	1
initial PCR activation	5 min	95°C	1
denaturation	15 sec	94°C	45
annealing & elongation	1 min	60°C *(TMPRSS2:ERG* 62°C)	

Reference genes standard curves

For comparative $\Delta\Delta C_t$ calculation, the PCR efficiency of target and reference genes must be approximately equal. This can be assured by amplifying a 10-fold RNA dilution series of target and reference gene. The template dilutions are plotted logarithmically against the cycle number (C_t) required to reach a pre-defined intensity threshold. Linear regression lines generate the so-called standard curves. The obtained slope gradients of the standard curves correlate with the PCR efficiencies and should not exceed 0.1 units for target and

control gene. The coefficient of determination (R^2) for both curves should be higher than 0.99 to allow comparison of them. Within the present work, standard curves for the quantification of *PARP1* were established. Standard curves for all other genes (*MSMB*, *NCOA4*, *TIMM23*, *PARG*, and *TMPRSS2:ERG*) were kindly provided by Dr. Manuel Lüdeke and Dr. Antje Rinckleb [57, 78]. Trend line equations for target and control genes were calculated using Microsoft Excel. Their slopes differed less than 0.1 and their coefficients of determination (R^2) were close to one, allowing a reliable calculation of relative expression levels.

The $\Delta\Delta C_t$ method

The $\Delta\Delta C_t$ method is used to calculate relative changes in the expression of a gene of interest in a sample of interest (normally a cDNA template) compared to a reference sample (e.g. cDNA from untreated cells). The housekeeping gene glucose-6-phosphate dehydrogenase *(G6PD)* was chosen as reference gene for the targets *MSMB*, *NCOA4*, *TIMM23*, *PARG* and *PARP1*. *TMPRSS2:ERG* was quantified as the outcome of the fusion gene induction assay. For this androgen-dependent transcript, expression of *TMPRSS2* was used as reference gene compensating androgen fluctuations. All target gene quantifications were performed in duplicates or triplicates, all outcome fusion quantifications in quadruplicates. Assuming that the PCR efficiency is close to 100%, the concentration of the amplified DNA and thus the fluorescence intensity increases exponentially. The threshold cycle C_t marks the point where the generated fluorescence is higher than the background level. It is empirically determined for each amplicon and should be within the exponential phase of curve. The relative expression of a gene of interest (relative to the reference gene) in a sample of interest relative to a reference sample can be calculated with the $\Delta\Delta C_t$ method. **Table 5** shows the experimental set-up for the calculation of relative expression levels.

Table 5: Experimental set-up for the calculation of relative expression levels. The relative expression of a gene of interest can be calculated with the mean cycle number value of the gene of interest (**gene a**) and the reference gene (**control b**) in the sample of interest and in the reference sample. Abbreviations: C_t = cycle number, ***ref*** = reference sample, siAllStars Control = validated negative control siRNA, ***SOI*** = sample of interest.

	Sample of interest ***SOI*** cells transfected with specific siRNA	**Reference sample** ***ref*** cells transfected with siAllStars Control
gene a	mean C_t (**gene a**;***SOI***)	mean C_t (**gene a**;***ref***)
control b	mean C_t (**control b**;***SOI***)	mean C_t (**control b**;***ref***)

First, the cycle C_t value differences (ΔC_t) between the gene of interest (**gene a**) and the reference gene (**control b**) have to be calculated in the sample of interest (***SOI***) and in the reference sample (***ref***).

ΔC_t (**gene a**;***SOI***) = mean C_t (**gene a**;***SOI***) - mean C_t (**control b**;***SOI***) (equation 1)

ΔC_t (**gene a**;***ref***) = mean C_t (**gene a**;***ref***) - mean C_t (**control b**;***ref***) (equation 2)

To reference the ΔC_t values of the target gene in the sample of interest (ΔC_t (**gene a**;***SOI***)) and in the reference sample (ΔC_t (**gene a**;***ref***)), ΔC_t values have to be subtracted.

$\Delta\Delta C_t = \Delta C_t$ (***gene a***;***SOI***) - ΔC_t (***gene a***;***ref***) (equation 3)

As the efficacy of target amplification is close to one, the fluorescence intensity increases exponentially. Hence, the relative expression of the target (*Q*) can be obtained by the following equation.

$Q = 2^{-\Delta\Delta Ct}$ (equation 4)

Some of the *TMPRSS2:ERG* measurements failed to be quantified by the ViiA™ 7 Real-Time PCR Software (Applied Biosystems, Life Technologies, Carlsbad, USA). Therefore, the relative *TMPRSS2:ERG* expression had to be corrected by the formula:

$$Q\ corrected = 2^{-\Delta\Delta Ct} \times \frac{number\ of\ valid\ quantifications}{number\ of\ total\ quantifications} \quad \text{(equation 5)}$$

All amplifications arising from very weak signals with threshold cycles above 37 were empirically considered as negative. Their amplification curve did not reach the threshold

cycle in the necessary logarithmic phase of amplification.

2.2.5. *TMPRSS2:ERG* induction assay

Backgrounds

Lin *et al.* established a cellular model to generate *de novo TMPRSS2:ERG* fusions in prostate cancer cells. Androgens and genotoxic stress synergistically induced prostate-cancer specific translocations [51]. Treatment with dihydrotestosterone (DHT) led to an androgen receptor dependent colocalization of *TMPRSS* and *ERG*. A following DNA damage pulse (γ-radiation) induced site-specific breakpoints within both genes. Consequentially, erroneous religation of fragmented DNA strands generated quantifiable *TMPRSS2:ERG* fusions [51]. Prostate cancer cells showed a preferable usage of the error-prone non-homologous end joining (NHEJ) repair pathway instead of the precise homologous recombination (HR). Insufficiencies in the DNA repair capacity facilitate the generation of unrepaired DNA double strand breaks, suggesting the NHEJ as major mechanism to generate *TMPRSS2:ERG* fusions [51].

Experimental procedure

In preparation for the induction of chromosomal translocations, LNCaP cells were first transfected with the respective target siRNA in hormone-reduced culture media. Thus, the addition of defined hormone doses was guaranteed. 90 minutes before irradiation, cells were stimulated with 1 µM DHT. Then, they were exposed to 300 Gray of γ-radiation in a caesium-137 source. After treatment, the cells were reincubated for 48 h in hormone-reduced media containing 1 µM DHT. During this incubation period, cells initialized their DNA repair processes and expressed the *TMPRSS2:ERG* fusion gene. Thereafter, cells were harvested for RNA isolation. The relative amount of *TMPRSS2:ERG* fusion transcript was quantified by qRT-PCR and normalized to the expression level of *TMPRSS2*. Negative and positive control experiments were routinely carried out in each experimental series. The negative control cells (mock) were transfected with a validated control siRNA (siAllStars Negative Control), the positive control cells with ESCO1 siRNA. Down-regulation of *ESCO1* within the *TMPRSS2:ERG* induction assay had already shown to generate significantly more *TMPRSS2:ERG* fusions [57]. The protocol for hormonal stimulation, γ-radiation and outcome fusion quantification used for the experimental cells was equally applied on the control cells.

To assure gene expression was silenced at the time of irradiation and fusion induction, knock-down control cells were transfected with the respective target siRNA. They were grown for 72 h in hormone-reduced culture medium and then harvested for target gene expression analysis. Quantification of the genes' relative expression levels revealed the siRNA knock-down efficacies at the time of fusion induction.

Untransfected cells guaranteed that the fusion depended on radiation and had not occurred before treatment. Cells were grown for 72 h in hormone-reduced culture medium and were then treated with 1 µM DHT. After 120 h they were harvested for *TMPRSS2:ERG* outcome expression analysis. A schematic overview of the experimental procedure is given in **Figure 2**.

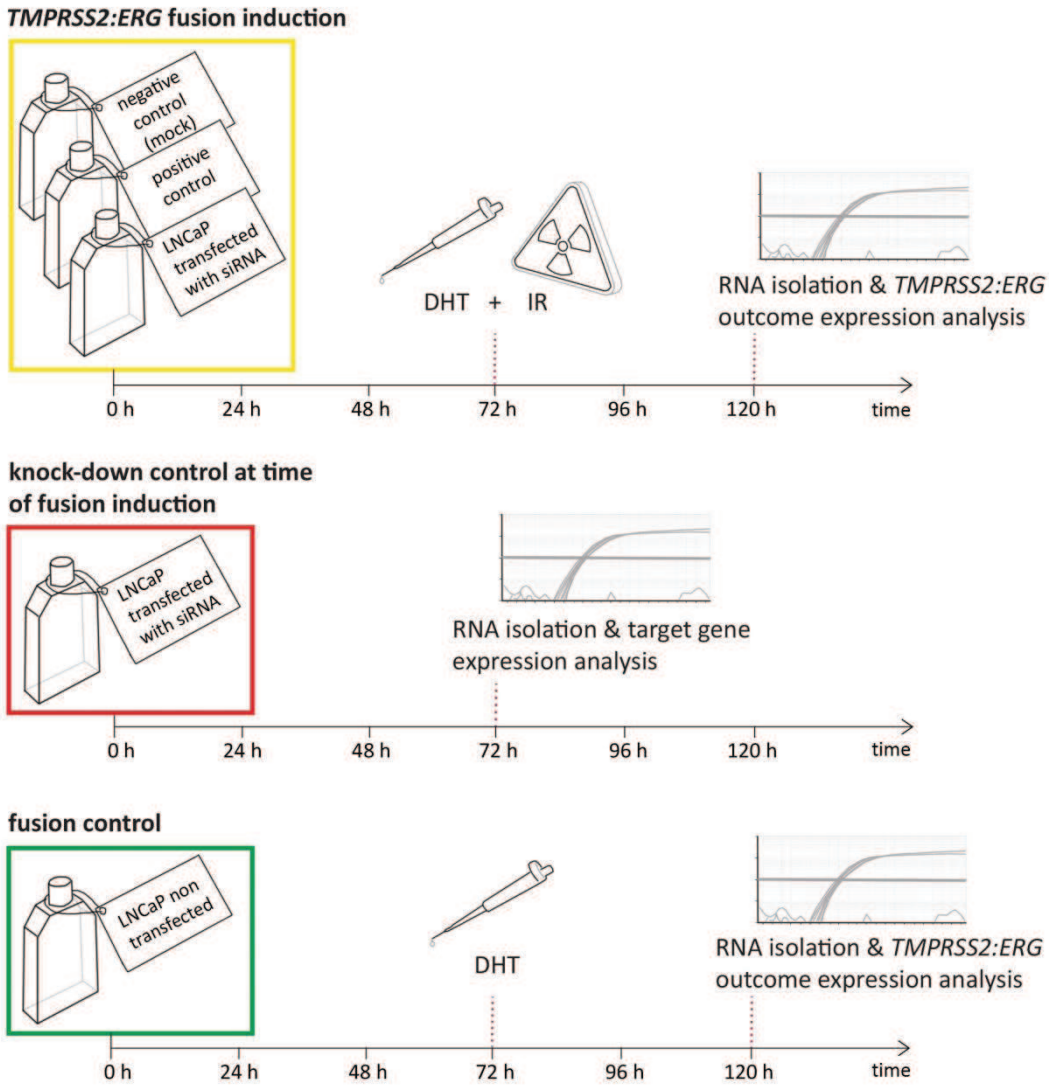

Figure 2: Schematic overview of the experimental procedure. *Yellow box*: Cells of the human prostate cancer cell line LNCaP were transfected with the particular target siRNAs, with a positive control and a negative control siRNA (mock). After 72 hours, all three approaches were treated with dihydrotestosterone and irradiated with 300 Gray. 120 hours after transfection, cells were harvested for RNA isolation and *TMPRSS2:ERG* gene expression analysis. *Red box*: The

knock-down control cells were transfected with the particular target siRNAs to assure effective down-regulation of the target's gene expression at the time of fusion induction (72 hours after transfection). *Green box*: The fusion control cells were treated with dihydrotestosterone only to guarantee that the generation of fusions depended on radiation. 120 hours after transfection cells were harvested for RNA isolation and *TMPRSS2:ERG* gene expression analysis. Abbreviations: DHT = dihydrotestosterone, h = hours, IR = irradiation, LNCaP = human prostate cancer cell line, *TMPRSS2:ERG* = gene symbol for the rearrangement between the genes *TMPRSS2* and *ERG*.

2.2.6. MTT-viability test

The MTT-viability test is a colorimetric assay to measure the redox-status of living cells [64]. NAD(P)H-dependent oxidoreductases in the mitochondria reduce the yellow tetrazolium MTT salt (3-(4,5-dimethylthiazol-2-yl)-2,5-diphenyl-tetrazoliumbromide) to the insoluble purple formazan. As the reduction only occurs in living cells, the concentration of formazan is proportional to the number of viable cells [18].

In the present work, the MTT viability assay was used to monitor the toxic effects of siRNA treatment on LNCaP cells. 120.000 cells per ml were grown in a 6-well plate and transfected with five different siRNA concentrations. To each well, 543 µl of MTT dye were added. Cells were incubated for 45 minutes. The supernatant was removed and 2.715 ml of MTT lysis buffer were added. Cells were briefly incubated at room temperature and then mixed on a shaker for 5 more minutes. From each cell culture plate eight aliquots of 100 µl were transferred to a 96-well plate for automatic photometric measurement. Absorbance was measured in octuplets at a wavelength of $\lambda = 570$ nm and referenced to cells transfected with siAllStars Negative Control.

2.2.7. Statistical analysis

The unpaired, heteroscedastic, two-sided t-test was used for all statistical analyses. The heteroscedastic t-test was applied because the comparative expression levels of target and reference genes had inhomogeneous variances. The 5% alpha-level (α) determined statistical significance ($p\text{-value} < 0.05$). Statistical parameters were calculated using Microsoft Excel.

3. Results

The prostate cancer risk variant rs10993994 has been associated with impairments in the cellular DNA repair capacity and with the *TMPRSS2:ERG* fusion positive prostate cancer. Considering that unrepaired DNA double strand breaks promote the generation of oncogenic rearrangements, the present work is based on the hypothesis that the mechanism of risk elevation conferred by the variant is an error-prone double strand break repair. Since a causative gene for the assumed pathomechanism is not yet identified, the candidate genes *MSMB*, *NCOA4*, *TIMM23* and *PARG* in 10q11 were tested on their effects on the formation of *TMPRSS2:ERG* fusions. It was also investigated if the functional opponent of *PARG, PARP1*, intervenes in the DNA repair and subsequently predisposes for the formation of *TMPRSS2:ERG* fusions. Therefore, the target gene expressions were silenced through siRNA and fusions were generated within the *TMPRSS2:ERG* induction assay. For test validity, down-regulation of *ESCO1*, which had already shown to induce significantly more *TMPRSS2:ERG* fusion in a similar experimental set-up was used as positive control.

3.1. Influence of down-regulation of *MSMB, NCOA4, TIMM23* and *PARG* on the generation of *TMPRSS2:ERG* fusions

3.1.1. Time response curves of target gene expression after siRNA transfection

All targetted gene expressions in siRNA transfected cells were quantified over a time period of 120 hours, generating time response curves (**Figure 3**). NCOA4, TIMM23 and PARG siRNA treatment revealed expression levels below 15% for the entire 120 hour time span (compared to siAllStar treated cells). The *MSMB* expression shortly increased after transfection, but decreased to residual values below 20% after 72 hours. Thereafter it remained steadily down-regulated. Since all candidate's expressions were certainly silenced 72 hours after transfection, this time point was chosen for the induction of *TMPRSS2:ERG* fusions. During the following incubation period of 48 h and before cell harvest (120 h after transfection), gene expressions were also reliably downregulated. A sufficient *ESCO1* knock-down had already been tested previously [57].

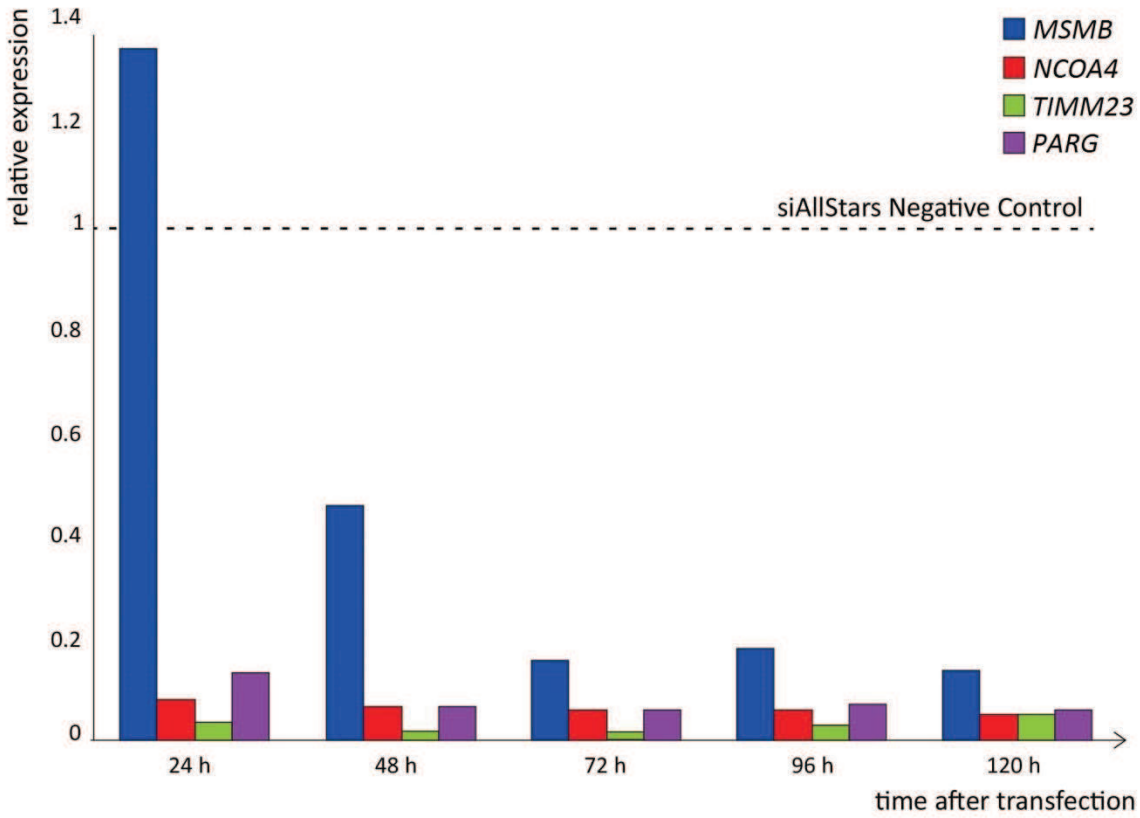

Figure 3: **Time response of target gene expression after siRNA transfection.** Cells of the human prostate cancer cell line LNCaP were transfected with siRNAs against *MSMB*, *NCOA4*, *TIMM23* and *PARG* or with the AllStars Negative Control siRNA. Target gene expressions were measured in lysates after 24, 48, 72, 96 and 120 hours and normalized on the reference gene *G6PD* (duplicates). The colored bars show the expression of the target genes *MSMB*, *NCOA4*, *TIMM23* and *PARG* relative to the respective gene expression in cells treated with a validated negative control siRNA. Abbreviations: h = hours, siAllStars Negative Control = validated negative control siRNA.

3.1.2. Dose-dependent effects of γ-radiation on *TMPRSS2:ERG* fusion induction and *TMPRSS2* expression

The protocol for the *TMPRSS2:ERG* induction assay had been determined by the time of fusion induction (72 h after transfection) and cell harvest (120 h after transfection). To establish the optimal quantity of γ-radiation for the induction of fusions, LNCaP cells were exposed to 50, 100, 200, 300 and 400 Gray in a caesium-137 source. 48 h after irradiation cells were harvested for *TMPRSS2:ERG* fusion quantifications. **Figure 4** shows the dose-dependent effect of γ-radiation on the *de novo* generation of fusions. Compared to the initial dose of 50 Gray, the number of *TMPRSS2:ERG* fusions increased with every dosage step. No fusions were observed in non-irradiated cells.

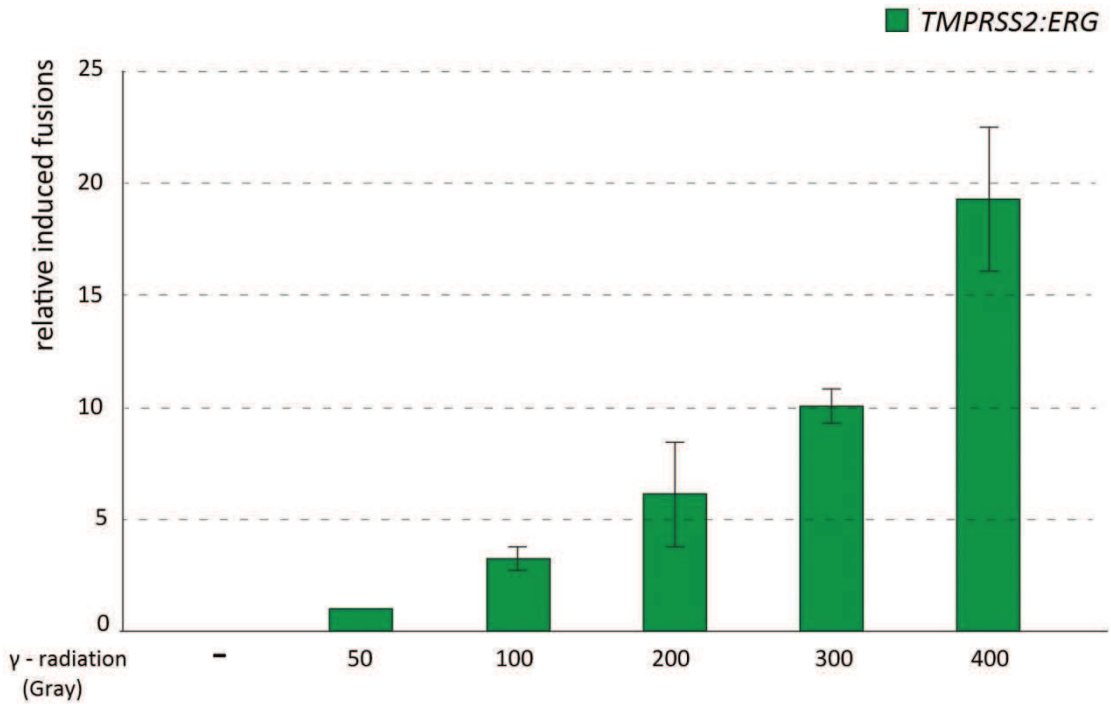

Figure 4: **Effect of γ-radiation on the induction of *TMPRSS2:ERG* gene fusions (n = 2, ± SEM).** Cells of the human prostate cancer cell line LNCaP were irradiated with 50, 100, 200, 300 and 400 Gray. *TMPRSS2:ERG* gene fusion transcripts were measured in lysates 48 hours after irradiation and normalized on the reference gene *TMPRSS2* (duplicates). The colored bars show the expression of *TMPRSS2:ERG* fusion transcripts relative to cells exposed to 50 Gray. Abbreviations: n = number of independent experiments, SEM = standard error of the mean.

Since the androgen-dependent promoter of *TMPRSS2* regulates the expression of *TMPRSS2:ERG* transcripts, the effect of γ-radiation on the *TMPRSS2* expression was assessed. LNCaP cells were exposed to 50, 100, 200, 300 and 400 Gray. 48 h after irradiation cells were harvested for the relative *TMPRSS2* expression quantification (**Figure 5**). Increasing radiation gradually suppressed *TMPRSS2* expression down to 23% of that in non-irradiated cells

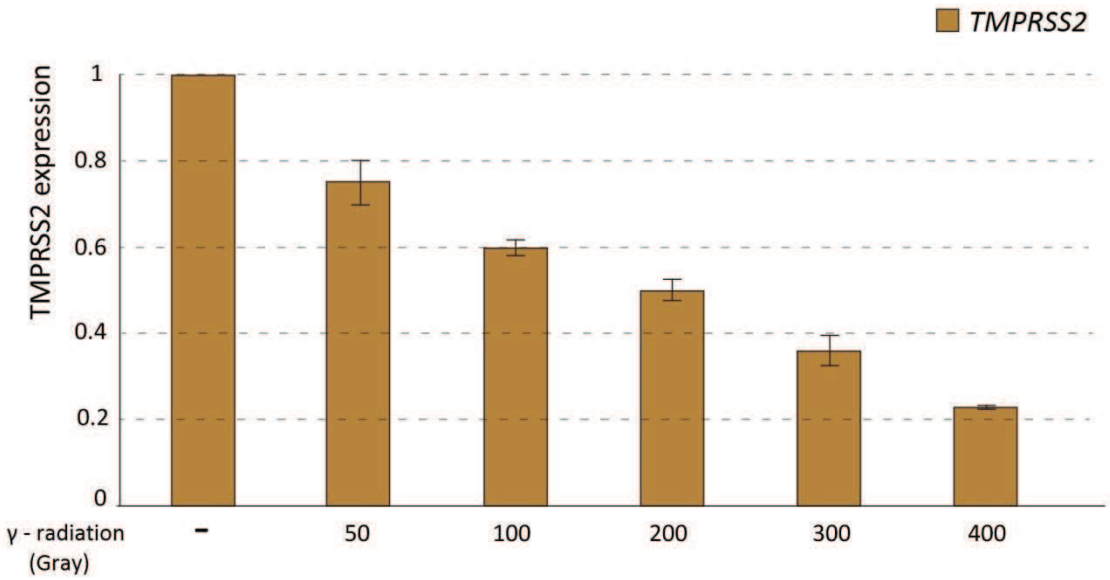

Figure 5: Effect of γ-radiation on *TMPRSS2* gene expression (n = 2, ± SEM). Cells of the human prostate cancer cell line LNCaP were irradiated with 50, 100, 200, 300 and 400 Gray. The *TMPRSS2* gene expression was measured in lysates 48 hours after irradiation and normalized on the reference gene *G6PD* (duplicates). The colored bars show the expression of *TMPRSS2* relative to non-irradiated cells. Abbreviations: n = number of independent experiments, SEM = standard error of the mean.

Because of the strong induction of fusions and the acceptable suppression of *TMPRSS2* at a radiation dose of 300 Gray, this dose was used in all further experiments.

3.1.3. Quantification of *de novo TMPRSS2:ERG* fusions after down-regulation of *MSMB*, *NCOA4*, *TIMM23* and *PARG*

After down-regulation of *MSMB*, *NCOA4*, *TIMM23* and *PARG, TMPRSS2:ERG* transcripts were quantified as outcome of the fusion induction assay in six individual experiments (**Figure 6**). The relative levels of *de novo* generated *TMPRSS2:ERG* fusions were obtained by referencing on cells treated with a validated negative control siRNA (siAllStars Negative Control). SiESCO1 treated cells served as positive control and non-transfected cells as fusion control to guarantee that the formation of fusions depended on radiation.

Silencing *PARG* led to a significant 3.0-fold increase in the formation of *TMPRSS2:ERG* fusions ($p = 0.001$). A slight but significant 1.8-fold enhanced number of fusions was also observed after down-regulation of *ESCO1* ($p = 0.025$). The knock-down of all other

evaluated genes did not significantly affect the formation of *TMPRSS2:ERG* fusions (*MSMB* 1.3-fold, p = 0.066; *NCOA4* 1.7-fold, p = 0.082, *TIMM23* 1.4-fold, p = 0.111).

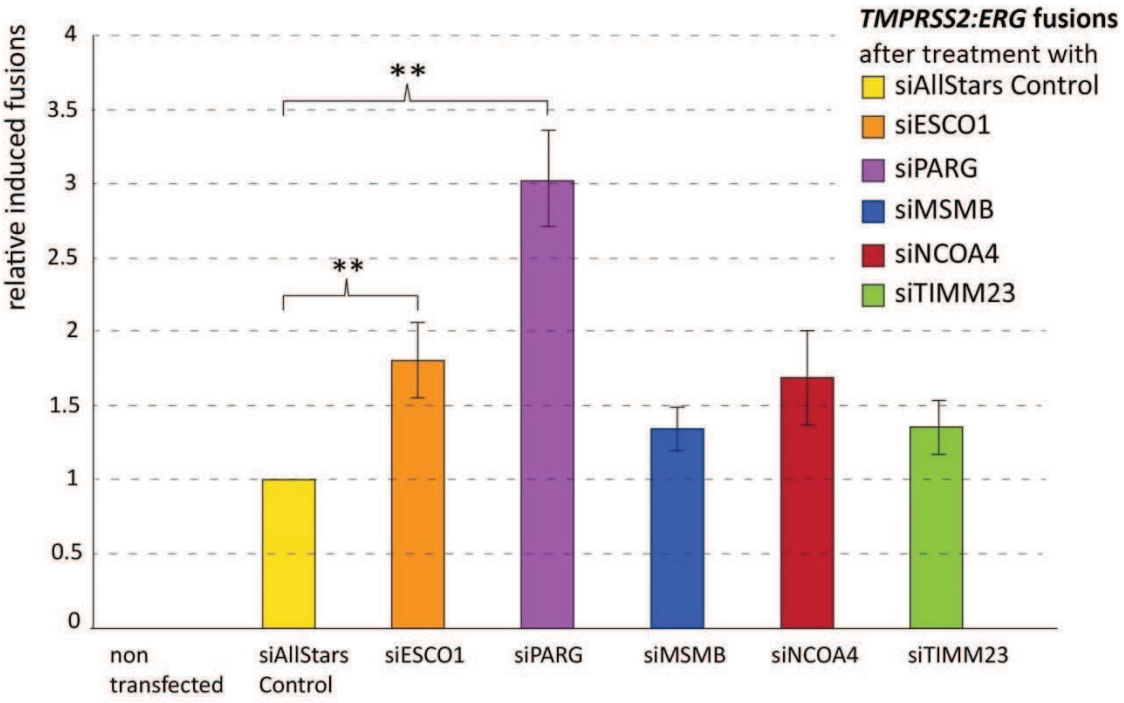

Figure 6: *TMPRSS2:ERG* fusion induction after silencing *ESCO1*, *PARG*, *MSMB*, *NCOA4* and *TIMM23* (n = 6, ± SEM, ** p < 0.05). Cells of the human prostate cancer cell line LNCaP were transfected with siRNAs against *ESCO1*, *PARG*, *MSMB*, *NCOA4* and *TIMM23* or with the AllStars Negative Control siRNA. 72 hours after transfection fusions were induced by hormonal stimulation and γ-radiation. After a recovery period of 48 hours, *TMPRSS2:ERG* gene fusion transcripts were measured in cell lysates and normalized on the reference gene *TMPRSS2* (quadruplicates). The colored bars show the relative induced *TMPRSS2:ERG* gene fusions relative to cells treated with the validated negative control siRNA. Abbreviations: n = number of independent experiments, SEM = standard error of the mean, siAllStars Control = validated negative control siRNA, siESCO1 = *ESCO1* specific siRNA, siMSMB = *MSMB* specific siRNA, siNCOA4 = *NCOA4* specific siRNA, siPARG = *PARG* specific siRNA, siTIMM23 = *TIMM23* specific siRNA.

The target gene expressions after siRNA treatment and at the time of irradiation were 23.6% for *ESCO1*, 6.7% for *PARG*, 11.9% for *MSMB*, 9.2% for *NCOA4* and 2.3% for *TIMM23* (**Figure 7**).

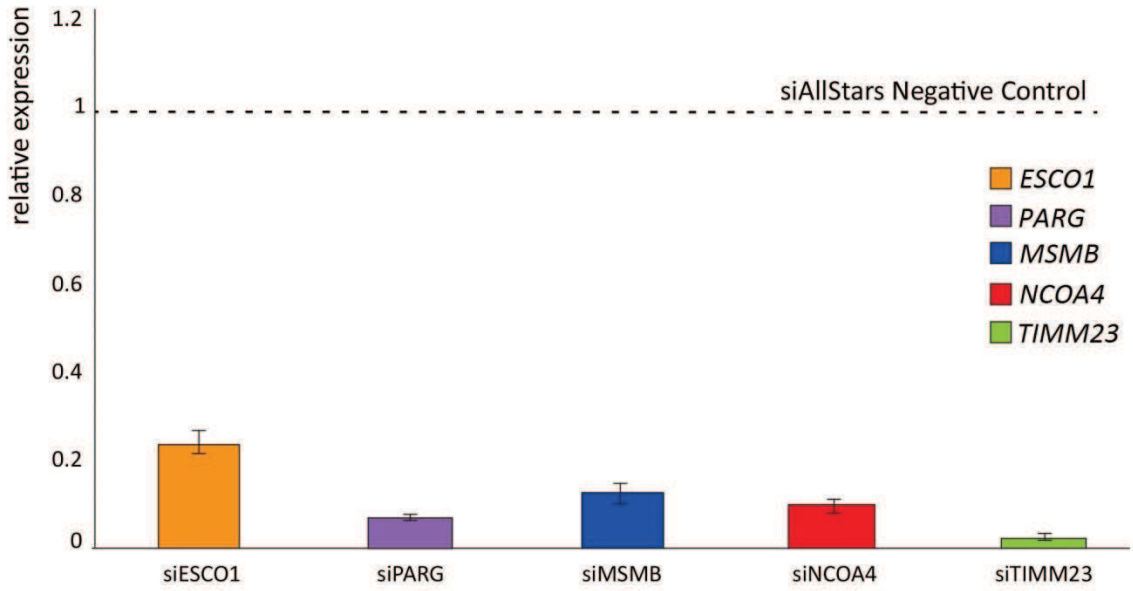

Figure 7: Target gene expression after siRNA treatment at time of irradiation (n = 6, ± SEM). Cells of the human prostate cancer cell line LNCaP were transfected with siRNAs against *ESCO1*, *PARG*, *MSMB*, *NCOA4* and *TIMM23* or with the AllStars Negative Control siRNA. Target gene expressions were measured in lysates after 72 hours and normalized on the reference gene *G6PD* (triplicates). The colored bars show the expression of the target genes *ESCO1*, *PARG*, *MSMB*, *NCOA4* and *TIMM23* relative to the respective gene expression in cells treated with a validated negative control siRNA. Abbreviations: n = number of independent experiments, SEM = standard error of the mean, siAllStars Negative Control = validated negative control siRNA, siESCO1 = *ESCO1* specific siRNA, siMSMB = *MSMB* specific siRNA, siNCOA4 = *NCOA4* specific siRNA, siPARG = *PARG* specific siRNA, siTIMM23 = *TIMM23* specific siRNA.

3.2. Influence of down-regulation of *PARP1* on the generation of *TMPRSS2:ERG* fusions

PARG and its functional opponent *PARP1,* directly influence the polymerization and cleavage of poly(ADP-ribose) branches in the cell by coordinated actions of their encoding enzymes. Since silencing *PARG* had already increased the number of *TMPRSS2:ERG* fusions, its counterpart *PARP1* was also down-regulated and tested on its effect on the formation of fusions.

3.2.1. Establishing PARP1 mRNA quantification

To validate the $\Delta\Delta C_t$ method, standard curves for *PARP1* and its reference gene *G6PD* were obtained in advance. A 10-fold dilution series of the *PARP1* and the *G6PD* RNA template concentrations were amplified and plotted against the number of cycles

required to reach the threshold cycle (C_t). The trend line equation and the coefficient of determination (R^2) for each regression line were calculated by using Microsoft Excel. As shown in **Figure 8**, the slope differences for both genes did not exceed 0.1 units and their coefficients of determination (R^2) were close to one. Therefore, both genes fulfill the prerequisites of the relative quantification method.

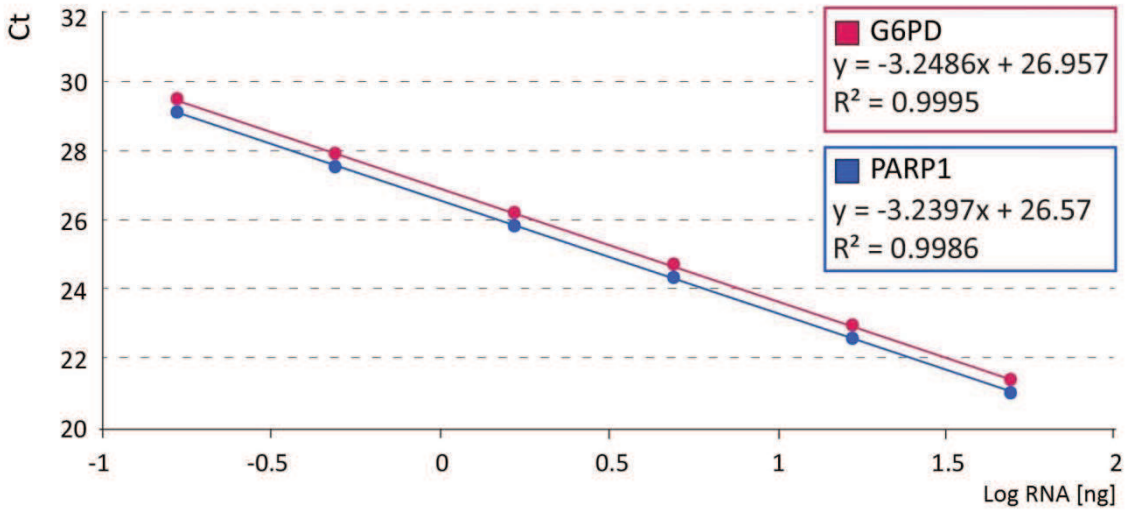

Figure 8: Standard curves for the target gene *PARP1* and the reference gene *G6PD*. Quantitative real-time PCR was performed with equidistant-concentrated RNA template from cells of the human prostate cancer cell line LNCaP. *PARP1* and *G6PD* RNA template concentrations were plotted against the number of cycles required to reach the threshold cycle, generating standard curves. Since the slope differences for both regression lines do not exceed 0.1 units and their correlation coefficient is close to one, relative expression levels can be calculated using the $\Delta\Delta C_t$ method. Amplifications were done in triplicates. Abbreviations: C_t = cycle number, Log = logarithm, ng = nanogram, R^2 = correlation coefficient.

3.2.2. Quantification of *de novo TMPRSS2:ERG* fusions at standard siPARP1 knock-down

According to protocol of the standard *TMPRSS2:ERG* induction assay, LNCaP cells were transfected with a 25 nM concentrated PARP1 siRNA. 72 hours after transfection and at the time of fusion induction, the siPARP1 treatment revealed a knock-down efficacy of 97% (data not shown). Silenced *PARP1* expression had no effect on the induction of *TMPRSS2:ERG* fusions (**Figure 9**). The number of generated fusions was very variable between individual experiments and did not significantly differ from the control cells (siAllStars Negative Control).

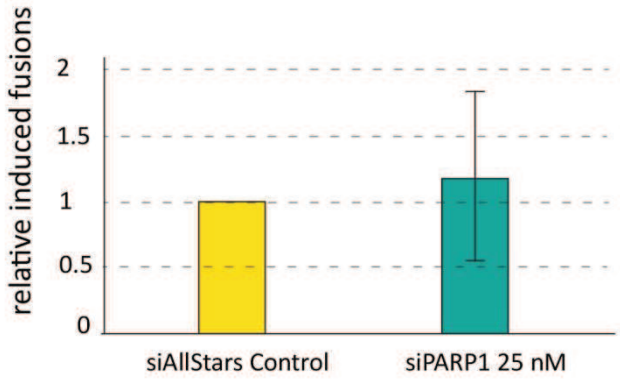

Figure 9: *TMPRSS2:ERG* fusion induction after silencing *PARP1* (n = 3, ± SEM). Cells of the human prostate cancer cell line LNCaP were transfected with a specific siRNA against *PARP1* or with the AllStars Negative Control siRNA. 72 hours after transfection fusions were induced by hormonal stimulation and γ-radiation. After a recovery period of 48 hours, *TMPRSS2:ERG* gene fusion transcripts were measured in cell lysates and normalized on the reference gene *TMPRSS2* (quadruplicates). The colored bars show the relative induced *TMPRSS2:ERG* gene fusions relative to cells treated with the validated negative control siRNA. Abbreviations: n = number of independent experiments, SEM = standard error of the mean, siAllStars Control = validated negative control siRNA, siPARP1 25 nM= *PARP1* specific siRNA in a concentration of 25 nanomolar.

3.2.3. Toxicity of siPARP1 treatment on LNCaP cells

To decrease the high variability in the outcome quantification of *TMPRSS2:ERG* fusions after siRNA transfection, the concentration dependent effect of the siPARP1 treatment on LNCaP cell viability was tested. Light microscopic examinations of siPARP1 treated cells revealed a high percentage of devitalized cells. To quantify the extent of cell death after transfection and at the time of fusion induction, LNCaP cells were exposed to decreasing siPARP1 concentrations. 72 hours after transfection, viability was assessed by using the MTT test. As shown in **Figure 10**, the standard siPARP1 treatment with a concentration of 25 nM impeded viability in more than 50% of cells, supporting the light microscopy appraisal. LNCaP cell survival increased with lower siRNA concentrations.

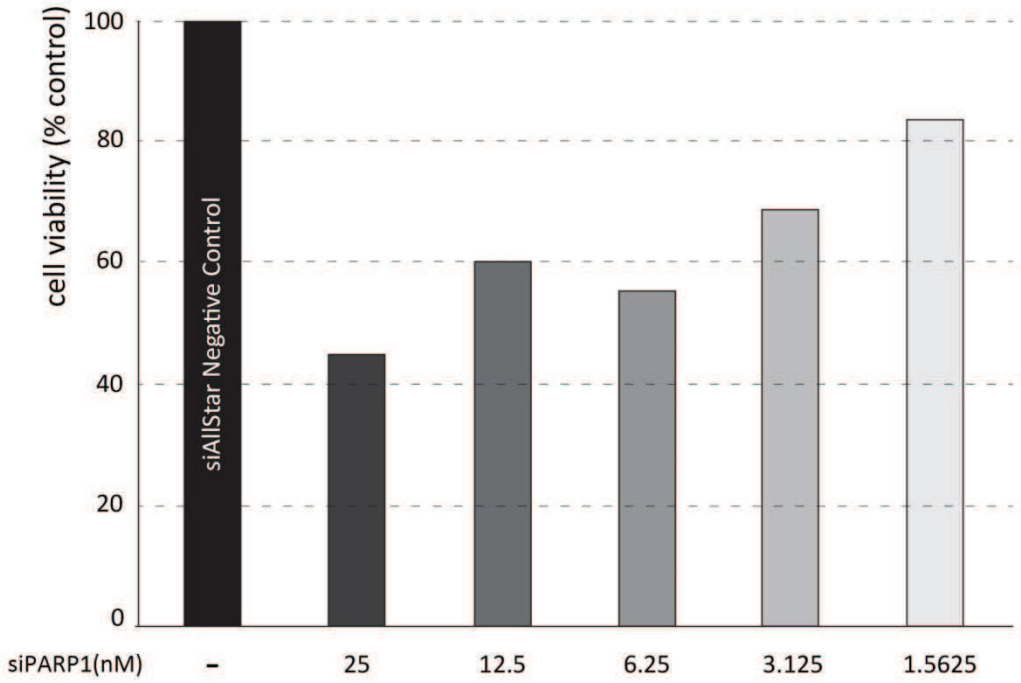

Figure 10: Concentration-dependent effects of *PARP1* siRNA knock-down on the cell viability. Cells of the human prostate cancer cell line LNCaP were transfected with decreasing concentrations of a specific siRNA against *PARP1* or with the AllStars Negative Control siRNA. 72 hours after transfection cell viability was assessed by using the MTT viability assay. The colored bars show the viability of cells treated with siRNA against *PARP1* compared to cells treated with a validated negative control siRNA (octuplets). Abbreviations: nM = nanomolar, siAllStars Negative Control = validated negative control siRNA, siPARP1 = *PARP1* specific siRNA, % control = percentage of control.

To correlate the increase in cell survival with the extent of *PARP1* depletion, the *PARP1* expression levels after siRNA treatment were quantified 72 hours after transfection for each siRNA concentration (**Figure 11**). The standard transfection with the 25 nM concentrated siPARP1 led to a remaining *PARP1* expression of 2.35% compared to the control. The following dilution steps of the siPARP1 concentration showed similar silencing effects with remaining *PARP1* expression levels below 5%.

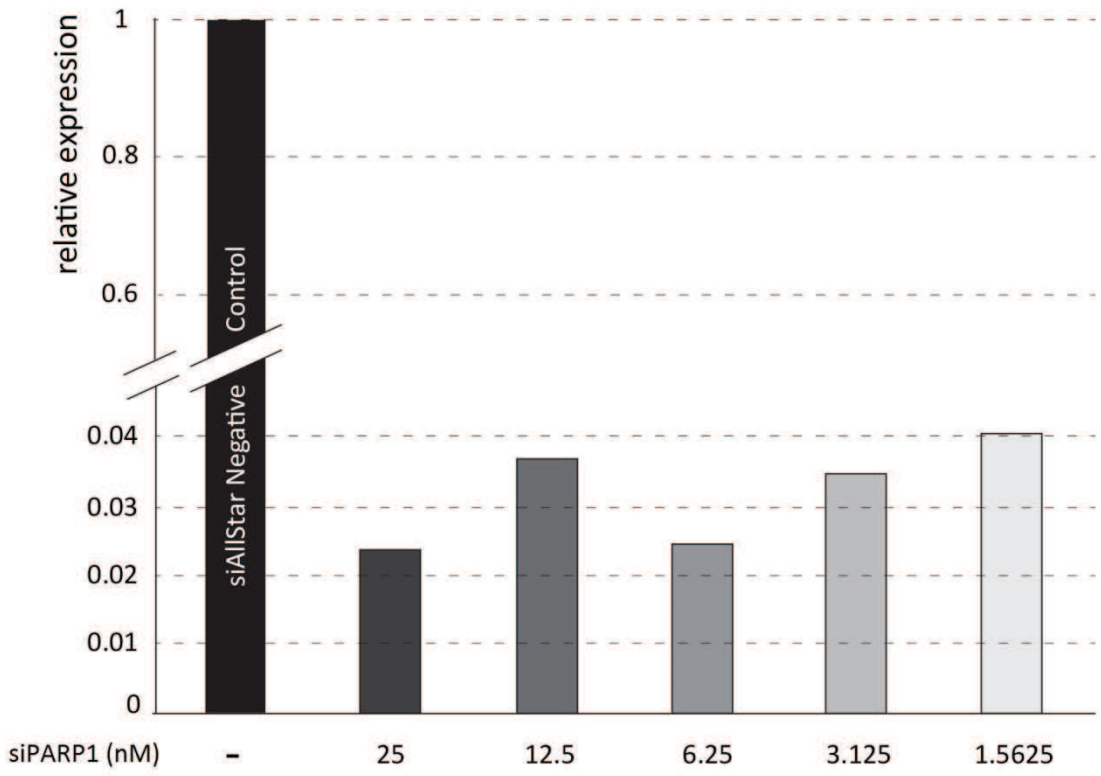

Figure 11: Concentration-dependent effects of *PARP1* siRNA knock-down on the *PARP1* gene expression. Cells of the human prostate cancer cell line LNCaP were transfected with decreasing concentrations of a specific siRNA against *PARP1* or with the AllStars Negative Control siRNA. *PARP1* gene expression was measured in cell lysates 72 hours after transfection and normalized on the reference gene *G6PD* (triplicates). The colored bars show the *PARP1* expression relative to cells treated with the validated negative control siRNA. Abbreviations: nM = nanomolar, siAllStars Negative Control = validated negative control siRNA, siPARP1 = *PARP1* specific siRNA.

Merged results for the concentration-dependent effects of siPARP1 on the cell viability and on the *PARP1* expression are shown in **Figure 12**. Transfection with 1.5625 nM concentrated siPARP1 yielded the best transfection tolerance and a maintained strong down-regulation of the *PARP1* expression. Therefore, this concentration was chosen for the transfection procedures in all further experiments.

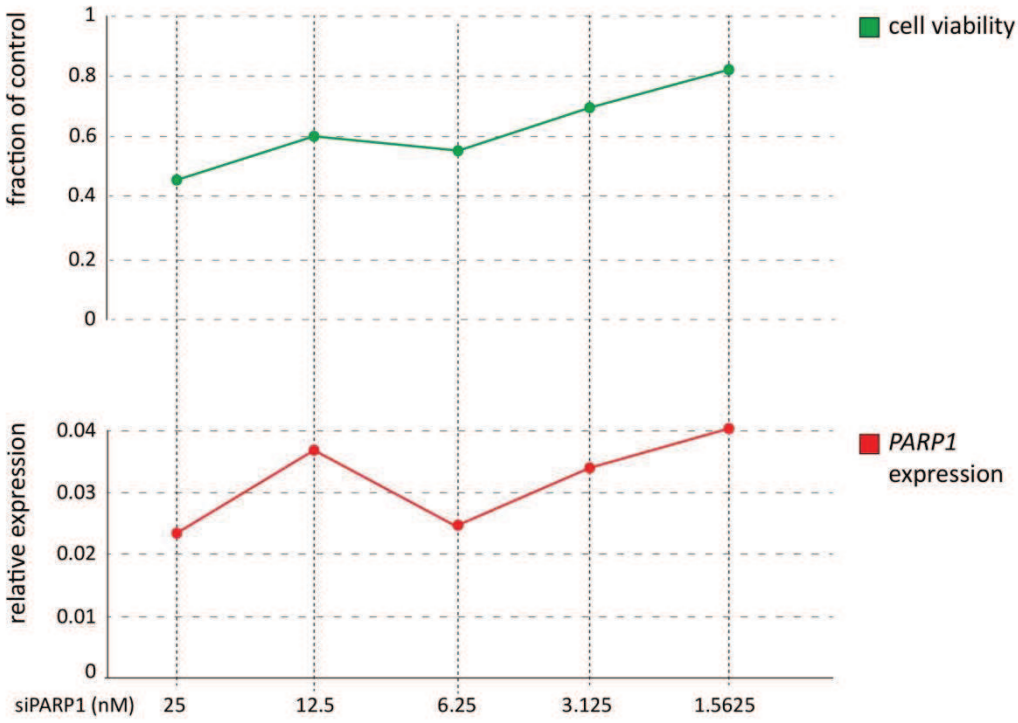

Figure 12: Merged results for cell viability and the *PARP1* gene expression after treatment with five different concentrations of a specific siRNA against *PARP1.* Cells of the human prostate cancer cell line LNCaP were transfected with decreasing siRNA concentrations against *PARP1*. The green line depicts the concentration-dependent effects of siRNA knock-down on the cell viability, the red line depicts the concentration-dependent effects of siRNA knock-down on the *PARP1* gene expression. Cell viability and *PARP1* gene expression were measured 72 hours after transfection. Abbreviations: nM = nanomolar, siPARP1 = *PARP1* specific siRNA.

3.2.4. Quantification of *de novo TMPRSS2:ERG* fusions at modified siPARP1 knock-down

The effect of a down-regulated *PARP1* expression on the formation of *TMPRSS2:ERG* fusions was tested with a lower siRNA concentration (1.5625 nM). The remaining *PARP1* expression at the time of fusion induction was 9.3% compared to the control (data not shown). Improved knock-down survival did not contribute to stabilize the variation in the fusion transcript quantifications (**Figure 13**). Thus, a final conclusion about the effect of a silenced *PARP1* expression on *TMPRSS2:ERG* fusions could not be drawn.

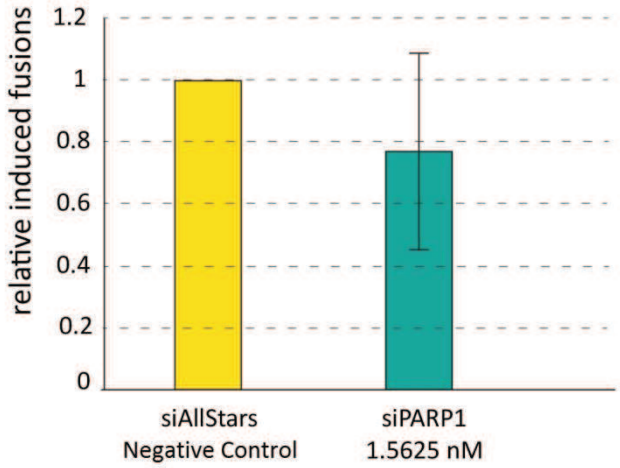

Figure 13: *TMPRSS2:ERG* fusion induction after silencing *PARP1* (n = 2, ± SEM). Cells of the human prostate cancer cell line LNCaP were transfected with a specific siRNA against *PARP1* or with the AllStars Negative Control siRNA. 72 hours after transfection fusions were induced by hormonal stimulation and γ-radiation. After a recovery period of 48 hours, *TMPRSS2:ERG* gene fusion transcripts were measured in cell lysates and normalized on the reference gene *TMPRSS2* (quadruplicates). The colored bars show the relative induced *TMPRSS2:ERG* gene fusions relative to cells treated with the validated negative control siRNA. Abbreviations: n = number of independent experiments, SEM = standard error of the mean, siAllStars Negative Control = validated negative control siRNA, siPARP1 1.5625 nM = *PARP1* specific siRNA in a concentration of 1.5625 nanomolar.

4. Discussion

Genome-wide association studies (GWAS) have identified more than 70 common susceptibility loci associated with prostate cancer risk. Despite prostate cancer has been the most successful of all cancers regarding the identification of susceptibility loci, little is known about the functional mechanisms that cause the observed risk increase [92]. Hence, the greatest challenge in the 'post-GWAS' era is to gain insights in how these individual germline variants confer disease susceptibility [27]. The present work is based on the mechanistical hypothesis that the prostate cancer variant rs10993994 in 10q11 exerts its risk increasing effect by an error-prone double strand break repair and therefore promotes oncogenic rearrangements. Previous work has suggested that the variant is related to an altered DNA repair capacity and is associated with the *TMPRSS2:ERG* fusion positive prostate cancer [78, 79]. The present study aim was to identify if any of the candidate genes *MSMB*, *NCOA4*, *TIMM23* and *PARG* in the direct surrounding of the variant is the causal perpetrator of the assumed pathomechanism. Therefore, all genes were analyzed on their functional implication in the generation of *TMPRSS2:ERG* fusions. As functional opponent of *PARG* and surrogate for a DNA repair regulator gene, *PARP1* was also tested on its effect on the formation of fusions.

The next sections will give a short overview over each candidate gene, its relevance in the pathogenesis of prostate cancer and in the generation of *TMPRSS2:ERG* fusions. Then, the *TMPRSS2:ERG* induction assay will be evaluated on advantages and limitations. The last sections will outline the importance of DNA repair and the *TMPRSS2:ERG* fusion for the development of prostate cancer.

4.1. Functional relevance of *MSMB*, *NCOA4*, *TIMM23* and *PARG* for the generation of *TMPRSS2:ERG* fusions in prostate cancer

Microseminoprotein beta (*MSMB*) or prostate secretory protein of 94 amino acids (PSP_{94})

Microseminoprotein beta (*MSMB*) encodes the prostate secretory protein of 94 amino acids (PSP_{94}). It is almost exclusively synthesized in the prostatic gland and is one of the

major components of the seminal fluid [50]. Several genome-wide association studies have identified the polymorphism rs10993994 in the 5' promoter region of *MSMB* as a prostate cancer risk variant [20, 41, 85]. Follow-up luciferase reporter and electrophoretic mobility shift assays revealed that the risk-associated T allele of the variant decreased the *MSMB* promoter activity due to a disrupted transcription factor binding site [11, 56]. The risk allele was further associated with decreased *MSMB* expression in benign and tumorigenic prostatic tissue and with lower protein concentrations in urine [74, 95]. Thus, increased prostate cancer risk is thought to be mediated by an altered *MSMB* expression.

MSMB/PSP_{94} levels in tumorigenic prostatic tissue have been found repeatedly decreased on both mRNA and protein level [10, 67, 81]. Therefore, the relevance of *MSMB* as a tumor suppressor gene has been undisputed. However, the exact mechanisms how *MSMB* exerts its inhibiting functions are not clear to date. Several studies using prostate cancer cell lines or animal xenograft models described a growth suppressing effect of *MSMB*/PSP_{94} on prostate cancer cells [28, 29, 54, 70, 82]. Furthermore, PSP_{94} seemed to antagonize tumor neovascularization by inhibition of the vascular endothelial growth factor 2 (VEGF-2) signaling pathway [43]. In the presence of PSP_{94} the VEGF-induced secretion of the matrix metalloproteinase 2 (MMP-2) was found decreased. MMPs are key enzymes in the process of matrix remodeling and crucial for tumor angiogenesis [43]. In contrast, loss of *MSMB* expression is thought to result in tumor-cell invasion and cancer progression [74].

The study aim of the present work was to identify whether *MSMB* influences the formation of *TMPRSS2:ERG* fusions and therefore predisposes for the development of prostate cancer. The results of the *TMPRSS2:ERG* induction assay revealed no significant effect of a silenced *MSMB* expression on the generation of fusions. This leads to the assumption that *MSMB* does not influence the formation of fusions and may therefore be discarded as causative candidate gene in 10q11. Although *MSMB* expression may be down-regulated by the local variant (rs10993994), the functional consequence of this mechanism is not reflected in an error-prone DNA repair and thus in the generation of oncogenic rearrangements. The presented data support a study of Rinckleb *et al.* who already questioned *MSMB* as the most plausible candidate gene for the prostate cancer

variant rs10993994. Blood lymphocytes carrying the T risk allele of the variant showed significant impairments in the DNA repair capacity, but did not express *MSMB* [79].

Nuclear receptor coactivator 4 (*NCOA4*) or androgen receptor associated protein 70 (ARA_{70})

NCOA4, which encodes the androgen receptor associated protein 70 (ARA_{70}), was first implicated in the pathogenesis of prostate cancer as co-activator of the androgen receptor [98]. *NCOA4* has two splicing variants, *NCOA4*α and *NCOA4*ß, which are located in different cellular compartments and seem to exert different functions [1]. *NCOA4*β-transfected prostate cancer cells showed enhanced proliferation and androgen-independent invasion through Matrigel [71]. In contrast, when *NCOA4*α was over-expressed proliferation, anchorage-independent growth and apoptosis were inhibited [47]. Studies examining the expressional status of *NCOA4* in prostatic tissue have yielded inconsistent results. Li *et al.* and Ligr *et al.* found a decreased expression of ARA_{70} in both high-grade prostate intraepithelial neoplasia (HGPIN) and in malignant cancer [47, 49]. In contrast, increased ARA_{70} levels in high-grade prostate cancer have also been described [37]. Finally, Mestayer *et al.* found no difference in the expression levels of *NCOA4* in tumorigenic compared to normal prostatic tissue [62].

Due to its localization close to the prostate cancer risk variant rs10993994, the expression of *NCOA4* has been correlated with the genotype status of the variant in tumorigenic and normal prostatic tissue. Pomerantz *et al.* found *NCOA4* expression genotype-dependent increased in histologically normal prostate tissue [74]. However, a second study could not replicate the described findings for *NCOA4* in normal tissue, but found a borderline increase in tumor tissue [78].

Belleli *et al.* recently characterized *NCOA4* as DNA replication regulator. *NCOA4* seems to block DNA replication at specific origin activation sides, hindering the CD45/MCM2-7/GINS (CMG)-helicase to unwind the DNA in preparation for replication [5]. Thus, *NCOA4* may control the spatial and temporal regulation of DNA replication, a feature that is often impaired in cancer cells [5]. Since the erroneous incorporation of bases during DNA replication needs a proficient DNA mismatch repair, loss of *NCOA4* may enhance unrepaired DNA damage and facilitate the emergence of oncogenic rearrangements.

To test whether *NCOA4* is in fact involved in error-prone DNA repair and subsequently predisposes for the generation of somatic rearrangements, the effect of a down-regulated *NCOA4* expression on the formation of *TMPRSS2:ERG* fusions was evaluated. The results of the *TMPRSS2:ERG* induction assay did not reveal an effect of *NCOA4* on the generation of fusions. These data suggest that *NCOA4* is not implicated in the DNA repair dependent susceptibility for developing prostate cancer and may therefore be ruled out as possible candidate gene in 10q11. Considering the conflicting studies about the *NCOA4* transcriptional status in prostate cancer, the question about a possible oncogenic or tumor inhibiting function of *NCOA4* remains unanswered. If and to what extend the variant rs10993994 is in fact capable of influencing *NCOA4* in its expression needs further evaluation.

Translocase of the inner mitochondrial membrane 23 (*TIMM23*)

TIMM23 (also known as *TIM23*) codes for a protein of the channel-forming pore of the Tim23 complex, an importer system of multiple precursor proteins into the mitochondrial matrix. Mitochondrial dysfunctions have long been an established feature of malignancy. Already in 1930, Warburg postulated that malignant cells generate energy from 'anaerobic glycolysis' due to insufficient mitochondrial respiration. Therefore, cancerous cells seem to adapt to hypoxic conditions better than healthy cells [91, 94].

Tim23 has been characterized as signaling molecule in the caspase-independent cell death. Cells induced to undergo apoptosis in the presence of caspase inhibitors seem to degrade Tim23 selectively [30]. Therefore, alterations in the expression levels of *TIMM23* may result in an insensitivity to apoptotic signals, a condition that promotes the malignant transformation of cells. Prostate cancer research has only focused on *TIMM23* in relation to the prostate cancer risk variant rs10993994. Due to its localization in 10q11, two studies have investigated if the risk-allele of the variant transcriptionally alters *TIMM23*. A first study did not find the *TIMM23* expression level associated with the genotype status in either normal or tumor tissue [74], whereas a second study found *TIMM23B* expression, the partial duplication of *TIMM23,* associated with the number of risk alleles in histologically normal prostatic tissue [78].

In the present work, *TIMM23* was evaluated on its putative involvement in the generation of *TMPRSS2:ERG* fusions and thus in the predisposition for developing prostate cancer.

Down-regulated *TIMM23* expression did not show to have an effect on the generation of fusions. Although *TIMM23* exhibits some tumorigenic characteristics, it seems not to be causative for the formation of oncogenic *TMPRSS2:ERG* fusions. Therefore, *TIMM23* may be discarded as candidate gene in 10q11. If the local variant confers prostate cancer risk by altering the *TIMM23* expression and if *TIMM23* and *TIMM23B* have segregated effects on the generation of fusions, still needs clarification.

Poly(ADP-ribose) glycohydrolase (*PARG*)

PARG, encoding the poly(ADP-ribose) glycohydrolase, is an important regulator of several cellular functions such as DNA replication and repair, post-transcriptional modification of proteins and cell death [16]. Together with its counterpart *PARP*, *PARG* tightly regulates the poly(ADP-ribose) metabolism. *PARP* transfers ADP-ribose from NAD^+ to a variety of target proteins, modifying their structure and function. Conversely, *PARG* restores the initial status by cleaving the protein-bound poly(ADP-ribose) polymers into single units. DNA damage enhances the poly(ADP-ribosylation) of a variety of DNA-associated proteins such as histones [61, 68], the DNA polymerase α, δ and ε [22] and *PARP1* itself [69]. After accomplished repair, *PARG* is involved in reconstituting the cell cycle. In fact, poly(ADP-ribose) polymers are found on a variety of cell-cycle checkpoint proteins [73] and are cleaved by *PARG* after accomplished DNA repair [16]. Therefore, *PARG* seems to inhibit the replication of damaged DNA, preserving the genomic integrity. Furthermore, *PARG* inhibition has shown to induce the collapse of DNA replication forks, requiring homologous recombination mediated repair [24].

With its importance in DNA repair and its localization in 10q11, *PARG* seems to be a promising candidate gene for the observed association between the rs10993994 and the DNA repair dependent prostate cancer risk mechanism. The results of the *TMPRSS2:ERG* induction assay revealed a significant 3.0-fold increase in the number of fusions after silencing *PARG* with siRNA ($p = 0.001$). This is the first evidence that *PARG* is causally involved in the emergence of *TMPRSS2:ERG* fusions in prostate cancer. The presented data supports *PARG* as the most plausible candidate gene in 10q11, mediating the risk-increasing effects of the local variant. Consistent with previous studies, *PARG* expression seems to be essential for the cellular ability to cope with genotoxic stress [13, 60]. An inhibition of *PARG* leads to a delayed DNA repair and a subsequent accumulation of

mitotic abnormalities [2]. These characteristics support that the prostate cancer variant rs10993994 may exert its risk conferring effect by inhibition of DNA repair (e.g. through silencing *PARG*) and thus promotes the generation of oncogenic rearrangements.

However, these finding have to be contemplated within some limitations. Uchiumi *et al*. found that silencing *PARG* in HeLa cells synergistically down-regulated the expression of its antagonist *PARP1* [90]. Hence, it is not sure that the observed increase in fusions results from *PARG* only. The effect of *PARG* on *TMPRSS2:ERG* fusions may be overestimated due to the effects of other deregulated genes. This phenomenon is probably not restricted to *PARP1*. *TIMM23* and *PARG* are also regulated in a common way as they have the same promoter [63]. Correlating the findings of the present work with the expressional status of *PARG* in tumorigenic tissue is somehow difficult. *PARG* mRNA levels in histologically malignant tissue were significantly up-regulated compared to normal prostatic tissue [78]. Therefore, it seems that both increased and decreased *PARG* expression levels are associated with malignant features of prostate cancer. This apparent contradiction may be explained by considering *PARG*'s function in the regulation of the poly(ADP-ribose) level. Silenced *PARG* expression has shown to increase the poly(ADP-ribose) level in the cell and on ribosylated proteins [34, 66]. This can be explained by the cleaving properties of its encoding enzyme, a glycohydrolase in charge of removing ADP-ribose from preexisting poly(ADP-ribose) branches. Considering now that both overexpression and down-regulation of *PARG* lead to alterations in the poly(ADP-ribose) level, the poly(ADP-ribose) homeostasis may as well be a general mechanism for prostate cancer susceptibility. In order to prove the previous hypothesis, overexpression of *PARG* and thus a depletion of the cellular poly(ADP-ribose) level needed to be tested on its effect on the formation of *TMPRSS2:ERG* fusions. Overexpressing *PARG* however, has so far been technically impossible, as LNCaP cells are not suitable for plasmid transfection. Therefore, *PARG*'s functional antagonist *PARP1* was down-regulated within the *TMPRSS2:ERG* induction assay and tested on putative effects on the generation of fusions. Like *PARG*, *PARP1* controls a proficient DNA repair and thus constitutes a surrogate for a DNA repair regulator gene.

4.2. Functional relevance of *PARP1* and the poly(ADP-ribose) level for the generation of *TMPRSS2:ERG* fusions in prostate cancer

PARP1 is the predominant enzyme of the poly(ADP-ribose) polymerase family in charge of synthesizing poly(ADP-ribose) from NAD^+. It is involved in the regulation of DNA repair, transcription and many other cellular processes [15, 102]. As a marker of apoptosis, *PARP1* is cleaved by caspases in programmed cell death [46, 99]. *PARP1* was chosen to be investigated in the present work to assess if alterations in the cellular level of poly(ADP-ribose) may influence the occurrence of *TMPRSS2:ERG* fusions. Noteworthy, down-regulation of *PARG*, the opposite regulator of the poly(ADP-ribose) equilibrium, had already shown to induce more fusions. Furthermore, *PARP1* is a regulator of DNA repair and therefore a promising candidate gene for the presumed DNA repair dependent mechanism for inherited prostate cancer risk.

The first results of the *TMPRSS2:ERG* induction assay revealed no significant effect of a silenced *PARP1* expression of the generation of fusions. Cell viability was importantly decreased by the transfection procedures, explaining the high variation in fusion quantifications between individual experiments. To reduce the variability of outcome quantifications, a modified knock-down protocol was applied. Cells were transfected with a lower concentrated siRNA, increasing viability at a maintained knock-down efficacy. However, the variation in the quantification of fusion transcripts remained high. Once again, silencing *PARP1* did not have a significant effect on the generation of *TMPRSS2:ERG* fusions.

Supporting previous studies on the radio sensitizing effect of *PARP1* inhibition on prostate cancer cell viability, the combination treatment of γ-radiation and siRNA transfection seemed to be too toxic for LNCaP cells [75]. Therefore, the effects of *PARP1* could not be reliably investigated within the *TMPRSS2:ERG* induction assay. If and to what extend the poly(ADP-ribose) level is a general mechanism for the emergence of *TMPRSS2:ERG* fusions and for prostate cancer susceptibility remains unanswered. The importance of the poly(ADP-ribose) homeostasis needs to be investigated in a different cellular model to understand if it is in fact a causative mechanism for the DNA repair dependent mechanism of increased prostate cancer risk.

4.3. Advantages and limitations of the *TMPRSS2:ERG* induction assay

Lin *et al.* developed a cell-culture based model to induce *TMPRSS2:ERG* fusions in androgen-responsive prostate cancer cells. The combined hormonal and genotoxic treatment with γ-radiation induced an androgen-receptor dependent spatial proximity between *TMPRSS2* and *ERG* through the activation of the actin/myosin system. Following site-specific DNA double-strand breaks within the *TMPRSS2* and the *ERG* gene generated broken DNA fragments. These seemed to be religated in a novel configuration, producing *TMPRSS2:ERG* fusions [51]. In the context of the present work, the prerequisite for the analysis of *MSMB*, *NCOA4*, *TIMM23* and *PARG* within the *TMPRSS2:ERG* induction assay was a successful down-regulation of the candidate gene expressions at the time of fusion induction (72 hours after transfection) and for the following recovery period (72-120 hours after transfection). *NCOA4*, *TIMM23* and *PARG* expression was steadily silenced for the total time-period of 120 hours with successful knock-down efficacies of over 80% (see 3.1.3). Contrarily, *MSMB* was first overexpressed 24 hours after transfection. However, its expression declined down to 15% over the course of time. This may be due to the low expression of *MSMB* in LNCaP cells, making its expression levels prone to fluctuations. Thus, a different cell-culture model may be more adequate for the analysis of low abundant transcripts, such as *MSMB*. *PARP1* expression was also successfully down-regulated 72 hours after transfection and at the time of fusion induction. The remaining *PARP1* expression was below 10% in all performed experiments. It has to be considered, that remaining protein levels after all siRNA transfections may have a residual function. Previous studies quantifying the protein levels of PARG and PARP1 after siRNA transfection found them steadily decreased 48 and 96 hours after transfection, respectively [66, 96]. Unfortunately, no information for protein half-live of the other genes was available.

The results of the *TMPRSS2:ERG* induction assay highlighted *PARG* as the most promising candidate gene for the prostate cancer risk loci 10q11. *PARG* seems to be causally implicated in the emergence of *TMPRSS2:ERG* fusions as the down-regulation of its expression led to a significant 3.0-fold increase in the formation of fusions. Down-regulation of all other genes, with exception of *PARP1*, resulted in a non-significantly increase in the generation of fusions. It is not quite sure if the common increment in

fusion frequencies arises from *off-target* effects of the siRNA treatments or from the down-regulation of the target genes. Therefore, the expression levels of all candidate genes were analyzed by quantitative RT-PCR for each single gene knock-down (data not shown). Independently performed experiments showed a strong variation supporting the idea of naturally fluctuating expression levels. However, many of the genes in the 10q11 region share a common regulation. It has already been described that the promoter of *MSMB* regulates the expression levels of both *MSMB* and *NCOA4* synergistically, producing full-length *MSMB-NCOA4* transcripts [55]. Even if the siRNA itself does not bind to promoter regions, it may target these full-length transcripts and cause cross-reactions. If and to what extent these *off*-targets obscure the effects of the analyzed genes is still unclear. To avoid this phenomenon, further experiments will have to search for alternative silencing methods (e.g. genetically engineered knock-out organisms, etc.).

The *TMPRSS2:ERG* induction assay represented a suitable tool to analyze putative effects of *MSMB*, *NCOA4, TIMM23* and *PARG* on the generation of *TMPRSS2:ERG* fusions. Even though the *TMPRSS2:ERG* fusions could be reproducibly induced with high doses of γ-radiation, they still constitute a rare event occurring in only a small fraction of the treated cells. For *PARP1* however, the combination treatment of androgens and γ-radiation was not compatible with a robust induction of *TMPRSS2:ERG* fusions. A different cellular model or experimental set-up may help to understand if *PARP1* is in fact involved in the occurrence of *TMPRSS2:ERG* fusions and thus in prostate cancer susceptibility.

4.4. DNA repair and its implication in prostate cancer pathogenesis and in the generation of *TMPRSS2:ERG* fusions

Genetic alterations in prostate cancer seem to arise predominantly from a molecular reshuffling of the genome rather than from single base pair changes [6]. This process, termed chromoplexy, appears to produce large chains of somatic rearrangements that affect many genes and chromosomes simultaneously [4]. The DNA sequence seems to be interrupted at characteristic breakpoints producing broken DNA ends that are shuffled and religated in a novel configuration [6]. Chromoplexy seems to occur in a coordinated

process rather than through multiple, independent steps [4]. Interestingly, *ETS*-rearranged prostate cancers show more inter-chromosomal rearrangements than *ETS*-negative cancers with more chromosomes affected by one single event [4]. This genomic reshuffling process seems to arise predominantly in androgen-driven transcription hubs on multiple chromosomal loci that co-localize during the interphase. The resulting 'rearrangement chains' may reflect DNA damage processes related to the androgen receptor signaling [4]. Lesions arising early in tumorigenesis are more likely to be clonal and favor a rapid cellular growth than later ones [4]. In fact, one of the earliest detectable alterations in *ETS*-rearranged prostate cancers is the deletion of a 3 Mb region on chromosome 21q which induces the *TMPRSS2:ERG* fusion [4, 72]. This event is frequently observed in prostatic intraepithelial neoplasia (PIN) and may alter the normal prostate epithelial differentiation [83]. Following lesions in *TP53* or *CDKN1*B seem to promote cancer progression by evasion from growth suppressors, increasing genome instability and activating invasion [4, 14]. The loss of *PTEN* finally paves the way for the development of aggressive prostate cancer [8]. Remarkably, the *TMPRSS2:ERG* fusion in androgen-dependent cells may also arise from an altered DNA repair machinery, which religates broken DNA fragments in a wrong way. Androgens and γ-radiation seem to recruit enzymes, which catalyze DNA double strand breaks to known break points within the *TMPRSS* and the *ERG* gene [33, 51]. Furthermore, hormonally stimulated prostate cancer cells activate the error-prone non-homologous end joining (NHEJ) repair pathway by recruiting proteins such as Ku70/Ku80 and ataxia telangiectasia mutated protein (ATM) to the sides of androgen receptor binding [51].

4.5. Clinical relevance of *TMPRSS2:ERG* fusions in prostate cancer

The *TMPRSS2:ERG* fusion was first described in 2005 by Tomlins *et al.* [88]. Thereafter, translocations involving the androgen-regulated *TMPRSS2* and genes of the *ETS* transcription factor family were identified in over 50% of prostate cancer cases [77, 89]. The fusion event places the *ERG* proto-oncogene, a member of the ETS transcription factor family, under the control of the androgen-regulated promoter of *TMPRSS2*, thereby enhancing its expression.

Found in 20% of high-grade prostatic intraepithelial neoplasia (HGPIN), the fusion appears to be an early event in tumor development [9]. Having its own molecular pattern and a distinct phenotype, *ETS*-rearranged prostate cancers can be differentiated from *ETS*-negative cancers [65, 76]. Since the *TMPRSS2:ERG* fusion has not been found in benign prostatic tissue or any other cancer type [32, 53], it may be used for diagnostics. So far, it has been proposed as complementary biomarker to the serum prostate-specific antigen (PSA) [44, 45]. However, quantification of *TMPRSS2:ERG* is not suitable for primary screening programs since it is only found in around 50% of all prostate cancer cases. Nevertheless, it could help to identify high-risk patients with persistently elevated PSA levels, but negative biopsies [36]. An association between *TMPRSS2:ERG* and malignant prostate cancer in terms of a possible use in risk stratification is controversially discussed in the literature. Some studies correlated the fusion status with a higher Gleason score and with prostate cancer-specific death [17, 77]. Other studies found no significant correlation with the TNM staging system, recurrence or any other clinical feature [26, 80]. These differences in the presumed prognostic value of the fusion status may be due to a limited comparability between the studies. The obtained data was derived from different cohorts (population-based watchful-waiting cohorts, retrospective radical prostatectomy cohorts, etc.) with different inclusion and aggressiveness criteria as well as variable end-points. If and to what extend the *TMPRSS2:ERG* fusion status can predict the patient's clinical outcome is not clear to date. However, personalized medicine by means of individually adapted treatment regimens will be one of the major challenges of oncology in the future. Therefore, an extensive molecular profiling of each patient's cancer subtype could help to differentiate those patients who suffer from an indolent cancer from those that need immediate treatment. Further insights in the signaling pathways of ERG-rearranged prostate cancers could help to design ERG-targeting vaccines as well as to facilitate the search for inhibitors of the downstream ERG signaling cascade [40, 93].

4.6. Conclusions

The present work identified *PARG* as most promising candidate gene exerting the risk increasing effect of the prostate cancer variant rs10993994 in 10q11. By an error-prone

double strand break repair and the subsequent generation of *TMPRSS2:ERG* fusions, *PARG* seems to be capable of influencing prostate cancer susceptibility. Previous studies have shown that down-regulation of *PARG* increases the poly(ADP-ribose) level in the cell. This may be explained by the function of its encoding enzyme, a glycohydrolase in charge of removing ADP-ribose from preexisting poly(ADP-ribose) branches. Thus, not only down-regulation of *PARG* but also alterations in the poly(ADP-ribose) equilibrium may be causative for the observed risk increase. Since the effect of down-regulated *PARP1*, the opposite regulator of the poly(ADP-ribose) homeostasis, could not be reliably investigated within the *TMPRSS2:ERG* induction assay, further work is needed to understand if the poly(ADP-ribose) level is in fact a general mechanism for the emergence of *TMPRSS2:ERG* fusions. So far, the results of the present work contribute to the identification of functional mechanisms that may cause inherited susceptibility to develop prostate cancer.

5. Summary

Genome-wide association studies (GWAS) have identified the inherited variant rs10993994 in 10q11 as being associated with prostate cancer risk. Beyond this trait association, the variant was functionally correlated with an altered DNA repair capacity and with the *TMPRSS2:ERG* fusion positive prostate cancer. Since an error-prone DNA repair predisposes for the generation of chromosomal rearrangements, this relationship seems not to be arbitrary.

The present work was based on the hypothesis that the variant rs10993994 exerts its risk increasing effects by an error-prone double strand break repair, thus promoting oncogenic rearrangements. To find the causal perpetrator of the presumed pathomechanism, the candidate genes *MSMB*, *NCOA4*, *TIMM23* and *PARG* in 10q11 were tested on their functional implication in the generation of *TMPRSS2:ERG* fusions. *PARP1*, the negative regulator of *PARG,* was also tested on its effect on the formation of fusions.

According to the *TMPRSS2:ERG* induction assay, fusions were generated in prostate cancer cells by stimulation with dihydrotestosterone and γ-radiation. *TMPRSS2:ERG* fusion transcripts were quantified by quantitative Real Time-Polymerase Chain Reaction (qRT-PCR). Down-regulation of *PARG* using siRNA led to a significant 3.0-fold increase in the number of fusions, whereas down-regulation of the other candidate genes did not result in a significant effect on the formation of fusions. Since previous studies showed that silenced *PARG* expression increases the cellular poly(ADP-ribose) level, not only *PARG* but also alterations in the poly(ADP-ribose) equilibrium may cause the observed increase. However, down-regulation of *PARP1*, the opposite regulator of the poly(ADP-ribose) level, did not have a significant effect on the generation of fusions.

The results of this work provide the first experimental evidence for a causal implication of *PARG* in the generation of *TMPRSS2:ERG* fusions in prostate cancer. Supporting the hypothesis of error-prone DNA repair as causal mechanism for the observed risk increase, *PARG* may be transcriptionally influenced by the variant rs10993994, impairing a proficient DNA repair and predisposing for the generation of oncogenic rearrangements. The results of the present work contribute to the identification of functional mechanisms that may cause individually inherited susceptibility to prostate cancer.

6. Literature

1. Alen P, Claessens F, Schoenmakers E, Swinnen J V, Verhoeven G, Rombauts W, Peeters B: Interaction of the putative androgen receptor-specific coactivator ARA70/ELE1alpha with multiple steroid receptors and identification of an internally deleted ELE1beta isoform. Mol.Endocrinol. 13: 117-128 (1999)

2. Ame J C, Fouquerel E, Gauthier L R, Biard D, Boussin F D, Dantzer F, de Murcia G, Schreiber V: Radiation-induced mitotic catastrophe in PARG-deficient cells. J.Cell.Sci. 122: 1990-2002 (2009)

3. Andrabi S A, Kim N S, Yu S W, Wang H, Koh D W, Sasaki M, Klaus J A, Otsuka T, Zhang Z, Koehler R C, Hurn P D, Poirier G G, Dawson V L, Dawson T M: Poly(ADP-ribose) (PAR) polymer is a death signal. Proc.Natl.Acad.Sci.U.S.A. 103: 18308-18313 (2006)

4. Baca S C, Prandi D, Lawrence M S, Mosquera J M, Romanel A, Drier Y, Park K, Kitabayashi N, MacDonald T Y, Ghandi M, Van Allen E, Kryukov G V, Sboner A, Theurillat J P, Soong T D, Nickerson E, Auclair D, Tewari A, Beltran H, Onofrio R C, Boysen G, Guiducci C, Barbieri C E, Cibulskis K, Sivachenko A, Carter S L, Saksena G, Voet D, Ramos A H, Winckler W, Cipicchio M, Ardlie K, Kantoff P W, Berger M F, Gabriel S B, Golub T R, Meyerson M, Lander E S, Elemento O, Getz G, Demichelis F, Rubin M A, Garraway L A: Punctuated evolution of prostate cancer genomes. Cell 153: 666-677 (2013)

5. Bellelli R, Castellone M D, Guida T, Limongello R, Dathan N A, Merolla F, Cirafici A M, Affuso A, Masai H, Costanzo V, Grieco D, Fusco A, Santoro M, Carlomagno F: NCOA4 Transcriptional Coactivator Inhibits Activation of DNA Replication Origins. Mol.Cell 55: 123-137 (2014)

6. Berger M F, Lawrence M S, Demichelis F, Drier Y, Cibulskis K, Sivachenko A Y, Sboner A, Esgueva R, Pflueger D, Sougnez C, Onofrio R, Carter S L, Park K, Habegger L, Ambrogio L, Fennell T, Parkin M, Saksena G, Voet D, Ramos A H, Pugh T J, Wilkinson J, Fisher S, Winckler W, Mahan S, Ardlie K, Baldwin J, Simons J W, Kitabayashi N, MacDonald T Y, Kantoff P W, Chin L, Gabriel S B, Gerstein M B, Golub T R, Meyerson M, Tewari A, Lander E S, Getz G, Rubin M A, Garraway L A: The genomic complexity of primary human prostate cancer. Nature 470: 214-220 (2011)

7. Bruner D W, Moore D, Parlanti A, Dorgan J, Engstrom P: Relative risk of prostate cancer for men with affected relatives: systematic review and meta-analysis. Int.J.Cancer 107: 797-803 (2003)

8. Carver B S, Tran J, Gopalan A, Chen Z, Shaikh S, Carracedo A, Alimonti A, Nardella C, Varmeh S, Scardino P T, Cordon-Cardo C, Gerald W, Pandolfi P P: Aberrant ERG expression cooperates with loss of PTEN to promote cancer progression in the prostate. Nat.Genet. 41: 619-624 (2009)

9. Cerveira N, Ribeiro F R, Peixoto A, Costa V, Henrique R, Jeronimo C, Teixeira M R: TMPRSS2-ERG gene fusion causing ERG overexpression precedes chromosome

copy number changes in prostate carcinomas and paired HGPIN lesions. Neoplasia 8: 826-832 (2006)

10. Chan P S, Chan L W, Xuan J W, Chin J L, Choi H L, Chan F L: In situ hybridization study of PSP94 (prostatic secretory protein of 94 amino acids) expression in human prostates. Prostate 41: 99-109 (1999)

11. Chang B L, Cramer S D, Wiklund F, Isaacs S D, Stevens V L, Sun J, Smith S, Pruett K, Romero L M, Wiley K E, Kim S T, Zhu Y, Zhang Z, Hsu F C, Turner A R, Adolfsson J, Liu W, Kim J W, Duggan D, Carpten J, Zheng S L, Rodriguez C, Isaacs W B, Gronberg H, Xu J: Fine mapping association study and functional analysis implicate a SNP in MSMB at 10q11 as a causal variant for prostate cancer risk. Hum.Mol.Genet. 18: 1368-1375 (2009)

12. Clark J P, Cooper C S: ETS gene fusions in prostate cancer. Nat.Rev.Urol. 6: 429-439 (2009)

13. Cortes U, Tong W M, Coyle D L, Meyer-Ficca M L, Meyer R G, Petrilli V, Herceg Z, Jacobson E L, Jacobson M K, Wang Z Q: Depletion of the 110-kilodalton isoform of poly(ADP-ribose) glycohydrolase increases sensitivity to genotoxic and endotoxic stress in mice. Mol.Cell.Biol. 24: 7163-7178 (2004)

14. Couto S S, Cao M, Duarte P C, Banach-Petrosky W, Wang S, Romanienko P, Wu H, Cardiff R D, Abate-Shen C, Cunha G R: Simultaneous haploinsufficiency of Pten and Trp53 tumor suppressor genes accelerates tumorigenesis in a mouse model of prostate cancer. Differentiation 77: 103-111 (2009)

15. D'Amours D, Desnoyers S, D'Silva I, Poirier G G: Poly(ADP-ribosyl)ation reactions in the regulation of nuclear functions. Biochem.J. 342 (Pt 2): 249-268 (1999)

16. Davidovic L, Vodenicharov M, Affar E B, Poirier G G: Importance of poly(ADP-ribose) glycohydrolase in the control of poly(ADP-ribose) metabolism. Exp.Cell Res. 268: 7-13 (2001)

17. Demichelis F, Fall K, Perner S, Andren O, Schmidt F, Setlur S R, Hoshida Y, Mosquera J M, Pawitan Y, Lee C, Adami H O, Mucci L A, Kantoff P W, Andersson S O, Chinnaiyan A M, Johansson J E, Rubin M A: TMPRSS2:ERG gene fusion associated with lethal prostate cancer in a watchful waiting cohort. Oncogene 26: 4596-4599 (2007)

18. Denizot F, Lang R: Rapid colorimetric assay for cell growth and survival. Modifications to the tetrazolium dye procedure giving improved sensitivity and reliability. J.Immunol.Methods 89: 271-277 (1986)

19. Edwards S M, Kote-Jarai Z, Meitz J, Hamoudi R, Hope Q, Osin P, Jackson R, Southgate C, Singh R, Falconer A, Dearnaley D P, Ardern-Jones A, Murkin A, Dowe A, Kelly J, Williams S, Oram R, Stevens M, Teare D M, Ponder B A, Gayther S A, Easton D F, Eeles R A, Cancer Research UK/Bristish Prostate Group UK Familial Prostate Cancer Study Collaborators, British Association of Urological Surgeons Section of Oncology: Two

percent of men with early-onset prostate cancer harbor germline mutations in the BRCA2 gene. Am.J.Hum.Genet. 72: 1-12 (2003)

20. Eeles R A, Kote-Jarai Z, Giles G G, Olama A A, Guy M, Jugurnauth S K, Mulholland S, Leongamornlert D A, Edwards S M, Morrison J, Field H I, Southey M C, Severi G, Donovan J L, Hamdy F C, Dearnaley D P, Muir K R, Smith C, Bagnato M, Ardern-Jones A T, Hall A L, O'Brien L T, Gehr-Swain B N, Wilkinson R A, Cox A, Lewis S, Brown P M, Jhavar S G, Tymrakiewicz M, Lophatananon A, Bryant S L, UK Genetic Prostate Cancer Study Collaborators, British Association of Urological Surgeons' Section of Oncology, UK ProtecT Study Collaborators, Horwich A, Huddart R A, Khoo V S, Parker C C, Woodhouse C J, Thompson A, Christmas T, Ogden C, Fisher C, Jamieson C, Cooper C S, English D R, Hopper J L, Neal D E, Easton D F: Multiple newly identified loci associated with prostate cancer susceptibility. Nat.Genet. 40: 316-321 (2008)

21. Eeles R A, Olama A A, Benlloch S, Saunders E J, Leongamornlert D A, Tymrakiewicz M, Ghoussaini M, Luccarini C, Dennis J, Jugurnauth-Little S, Dadaev T, Neal D E, Hamdy F C, Donovan J L, Muir K, Giles G G, Severi G, Wiklund F, Gronberg H, Haiman C A, Schumacher F, Henderson B E, Le Marchand L, Lindstrom S, Kraft P, Hunter D J, Gapstur S, Chanock S J, Berndt S I, Albanes D, Andriole G, Schleutker J, Weischer M, Canzian F, Riboli E, Key T J, Travis R C, Campa D, Ingles S A, John E M, Hayes R B, Pharoah P D, Pashayan N, Khaw K T, Stanford J L, Ostrander E A, Signorello L B, Thibodeau S N, Schaid D, Maier C, Vogel W, Kibel A S, Cybulski C, Lubinski J, Cannon-Albright L, Brenner H, Park J Y, Kaneva R, Batra J, Spurdle A B, Clements J A, Teixeira M R, Dicks E, Lee A, Dunning A M, Baynes C, Conroy D, Maranian M J, Ahmed S, Govindasami K, Guy M, Wilkinson R A, Sawyer E J, Morgan A, Dearnaley D P, Horwich A, Huddart R A, Khoo V S, Parker C C, Van As N J, Woodhouse C J, Thompson A, Dudderidge T, Ogden C, Cooper C S, Lophatananon A, Cox A, Southey M C, Hopper J L, English D R, Aly M, Adolfsson J, Xu J, Zheng S L, Yeager M, Kaaks R, Diver W R, Gaudet M M, Stern M C, Corral R, Joshi A D, Shahabi A, Wahlfors T, Tammela T L, Auvinen A, Virtamo J, Klarskov P, Nordestgaard B G, Roder M A, Nielsen S F, Bojesen S E, Siddiq A, Fitzgerald L M, Kolb S, Kwon E M, Karyadi D M, Blot W J, Zheng W, Cai Q, McDonnell S K, Rinckleb A E, Drake B, Colditz G, Wokolorczyk D, Stephenson R A, Teerlink C, Muller H, Rothenbacher D, Sellers T A, Lin H Y, Slavov C, Mitev V, Lose F, Srinivasan S, Maia S, Paulo P, Lange E, Cooney K A, Antoniou A C, Vincent D, Bacot F, Tessier D C, COGS-Cancer Research UK GWAS-ELLIPSE (part of GAME-ON) Initiative, Australian Prostate Cancer Bioresource, UK Genetic Prostate Cancer Study Collaborators/British Association of Urological Surgeons' Section of Oncology, UK ProtecT (Prostate testing for cancer and Treatment) Study Collaborators, PRACTICAL (Prostate Cancer Association Group to Investigate Cancer-Associated Alterations in the Genome) Consortium, Kote-Jarai Z, Easton D F: Identification of 23 new prostate cancer susceptibility loci using the iCOGS custom genotyping array. Nat.Genet. 45: 385-91, 391e1-2 (2013)

22. Eki T: Poly (ADP-ribose) polymerase inhibits DNA replication by human replicative DNA polymerase alpha, delta and epsilon in vitro. FEBS Lett. 356: 261-266 (1994)

23. Ewing C M, Ray A M, Lange E M, Zuhlke K A, Robbins C M, Tembe W D, Wiley K E, Isaacs S D, Johng D, Wang Y, Bizon C, Yan G, Gielzak M, Partin A W, Shanmugam V,

Izatt T, Sinari S, Craig D W, Zheng S L, Walsh P C, Montie J E, Xu J, Carpten J D, Isaacs W B, Cooney K A: Germline mutations in HOXB13 and prostate-cancer risk. N.Engl.J.Med. 366: 141-149 (2012)

24. Fathers C, Drayton R M, Solovieva S, Bryant H E: Inhibition of poly(ADP-ribose) glycohydrolase (PARG) specifically kills BRCA2-deficient tumor cells. Cell.Cycle 11: 990-997 (2012)

25. Ferlay J, Soerjomataram I, Ervik M, Dikshit R, Eser S, Mathers C, Rebelo M, Parkin DM, Forman D, Bray, F.: GLOBOCAN 2012 v1.0, Cancer Incidence and Mortality Worldwide: IARC CancerBase No. 11 [Internet] Lyon, France: International Agency for Research on Cancer; 2013.

26. Fernandez-Serra A, Rubio L, Calatrava A, Rubio-Briones J, Salgado R, Gil-Benso R, Espinet B, Garcia-Casado Z, Lopez-Guerrero J A: Molecular characterization and clinical impact of TMPRSS2-ERG rearrangement on prostate cancer: comparison between FISH and RT-PCR. Biomed.Res.Int. 2013: 465179 (2013)

27. Freedman M L, Monteiro A N, Gayther S A, Coetzee G A, Risch A, Plass C, Casey G, De Biasi M, Carlson C, Duggan D, James M, Liu P, Tichelaar J W, Vikis H G, You M, Mills I G: Principles for the post-GWAS functional characterization of cancer risk loci. Nat.Genet. 43: 513-518 (2011)

28. Garde S, Sheth A, Porter A T, Pienta K J: Effect of prostatic inhibin peptide (PIP) on prostate cancer cell growth in vitro and in vivo. Prostate 22: 225-233 (1993)

29. Garde S V, Basrur V S, Li L, Finkelman M A, Krishan A, Wellham L, Ben-Josef E, Haddad M, Taylor J D, Porter A T, Tang D G: Prostate secretory protein (PSP94) suppresses the growth of androgen-independent prostate cancer cell line (PC3) and xenografts by inducing apoptosis. Prostate 38: 118-125 (1999)

30. Goemans C G, Boya P, Skirrow C J, Tolkovsky A M: Intra-mitochondrial degradation of Tim23 curtails the survival of cells rescued from apoptosis by caspase inhibitors. Cell Death Differ. 15: 545-554 (2008)

31. Goh C L, Schumacher F R, Easton D, Muir K, Henderson B, Kote-Jarai Z, Eeles R A: Genetic variants associated with predisposition to prostate cancer and potential clinical implications. J.Intern.Med. 271: 353-365 (2012)

32. Green W M, Hicks J L, De Marzo A, Illei P P, Epstein J I: Immunohistochemical evaluation of TMPRSS2-ERG gene fusion in adenosis of the prostate. Hum.Pathol. 44: 1895-1901 (2013)

33. Haffner M C, Aryee M J, Toubaji A, Esopi D M, Albadine R, Gurel B, Isaacs W B, Bova G S, Liu W, Xu J, Meeker A K, Netto G, De Marzo A M, Nelson W G, Yegnasubramanian S: Androgen-induced TOP2B-mediated double-strand breaks and prostate cancer gene rearrangements. Nat.Genet. 42: 668-675 (2010)

34. Hanai S, Kanai M, Ohashi S, Okamoto K, Yamada M, Takahashi H, Miwa M: Loss of poly(ADP-ribose) glycohydrolase causes progressive neurodegeneration in Drosophila melanogaster. Proc.Natl.Acad.Sci.U.S.A. 101: 82-86 (2004)

35. Hankey B F, Feuer E J, Clegg L X, Hayes R B, Legler J M, Prorok P C, Ries L A, Merrill R M, Kaplan R S: Cancer surveillance series: interpreting trends in prostate cancer--part I: Evidence of the effects of screening in recent prostate cancer incidence, mortality, and survival rates. J.Natl.Cancer Inst. 91: 1017-1024 (1999)

36. Hessels D, Smit F P, Verhaegh G W, Witjes J A, Cornel E B, Schalken J A: Detection of TMPRSS2-ERG fusion transcripts and prostate cancer antigen 3 in urinary sediments may improve diagnosis of prostate cancer. Clin.Cancer Res. 13: 5103-5108 (2007)

37. Hu Y C, Yeh S, Yeh S D, Sampson E R, Huang J, Li P, Hsu C L, Ting H J, Lin H K, Wang L, Kim E, Ni J, Chang C: Functional domain and motif analyses of androgen receptor coregulator ARA70 and its differential expression in prostate cancer. J.Biol.Chem. 279: 33438-33446 (2004)

38. International HapMap Consortium: The International HapMap Project. Nature 426: 789-796 (2003)

39. Jin G, Lu L, Cooney K A, Ray A M, Zuhlke K A, Lange E M, Cannon-Albright L A, Camp N J, Teerlink C C, Fitzgerald L M, Stanford J L, Wiley K E, Isaacs S D, Walsh P C, Foulkes W D, Giles G G, Hopper J L, Severi G, Eeles R, Easton D, Kote-Jarai Z, Guy M, Rinckleb A, Maier C, Vogel W, Cancel-Tassin G, Egrot C, Cussenot O, Thibodeau S N, McDonnell S K, Schaid D J, Wiklund F, Gronberg H, Emanuelsson M, Whittemore A S, Oakley-Girvan I, Hsieh C L, Wahlfors T, Tammela T, Schleutker J, Catalona W J, Zheng S L, Ostrander E A, Isaacs W B, Xu J, International Consortium for Prostate Cancer Genetics: Validation of prostate cancer risk-related loci identified from genome-wide association studies using family-based association analysis: evidence from the International Consortium for Prostate Cancer Genetics (ICPCG). Hum.Genet. 131: 1095-1103 (2012)

40. Kissick H T, Sanda M G, Dunn L K, Arredouani M S: Development of a peptide-based vaccine targeting TMPRSS2:ERG fusion-positive prostate cancer. Cancer Immunol.Immunother. 62: 1831-1840 (2013)

41. Kote-Jarai Z, Easton D F, Stanford J L, Ostrander E A, Schleutker J, Ingles S A, Schaid D, Thibodeau S, Dork T, Neal D, Donovan J, Hamdy F, Cox A, Maier C, Vogel W, Guy M, Muir K, Lophatananon A, Kedda M A, Spurdle A, Steginga S, John E M, Giles G, Hopper J, Chappuis P O, Hutter P, Foulkes W D, Hamel N, Salinas C A, Koopmeiners J S, Karyadi D M, Johanneson B, Wahlfors T, Tammela T L, Stern M C, Corral R, McDonnell S K, Schurmann P, Meyer A, Kuefer R, Leongamornlert D A, Tymrakiewicz M, Liu J F, O'Mara T, Gardiner R A, Aitken J, Joshi A D, Severi G, English D R, Southey M, Edwards S M, Al Olama A A, PRACTICAL Consortium, Eeles R A: Multiple novel prostate cancer predisposition loci confirmed by an international study: the PRACTICAL Consortium. Cancer Epidemiol.Biomarkers Prev. 17: 2052-2061 (2008)

42. Kote-Jarai Z, Leongamornlert D, Tymrakiewicz M, Field H, Guy M, Al Olama A A, Morrison J, O'Brien L, Wilkinson R, Hall A, Sawyer E, Muir K, Hamdy F, Donovan J, Neal D, Easton D, Eeles R: Mutation analysis of the MSMB gene in familial prostate cancer. Br.J.Cancer 102: 414-418 (2010)

43. Lamy S, Ruiz M T, Wisniewski J, Garde S, Rabbani S A, Panchal C, Wu J J, Annabi B: A prostate secretory protein94-derived synthetic peptide PCK3145 inhibits VEGF signalling in endothelial cells: implication in tumor angiogenesis. Int.J.Cancer 118: 2350-2358 (2006)

44. Laxman B, Morris D S, Yu J, Siddiqui J, Cao J, Mehra R, Lonigro R J, Tsodikov A, Wei J T, Tomlins S A, Chinnaiyan A M: A first-generation multiplex biomarker analysis of urine for the early detection of prostate cancer. Cancer Res. 68: 645-649 (2008)

45. Laxman B, Tomlins S A, Mehra R, Morris D S, Wang L, Helgeson B E, Shah R B, Rubin M A, Wei J T, Chinnaiyan A M: Noninvasive detection of TMPRSS2:ERG fusion transcripts in the urine of men with prostate cancer. Neoplasia 8: 885-888 (2006)

46. Lazebnik Y A, Kaufmann S H, Desnoyers S, Poirier G G, Earnshaw W C: Cleavage of poly(ADP-ribose) polymerase by a proteinase with properties like ICE. Nature 371: 346-347 (1994)

47. Li P, Yu X, Ge K, Melamed J, Roeder R G, Wang Z: Heterogeneous expression and functions of androgen receptor co-factors in primary prostate cancer. Am.J.Pathol. 161: 1467-1474 (2002)

48. Lichtenstein P, Holm N V, Verkasalo P K, Iliadou A, Kaprio J, Koskenvuo M, Pukkala E, Skytthe A, Hemminki K: Environmental and heritable factors in the causation of cancer--analyses of cohorts of twins from Sweden, Denmark, and Finland. N.Engl.J.Med. 343: 78-85 (2000)

49. Ligr M, Li Y, Zou X, Daniels G, Melamed J, Peng Y, Wang W, Wang J, Ostrer H, Pagano M, Wang Z, Garabedian M J, Lee P: Tumor suppressor function of androgen receptor coactivator ARA70alpha in prostate cancer. Am.J.Pathol. 176: 1891-1900 (2010)

50. Lilja H, Abrahamsson P A: Three predominant proteins secreted by the human prostate gland. Prostate 12: 29-38 (1988)

51. Lin C, Yang L, Tanasa B, Hutt K, Ju B G, Ohgi K, Zhang J, Rose D W, Fu X D, Glass C K, Rosenfeld M G: Nuclear receptor-induced chromosomal proximity and DNA breaks underlie specific translocations in cancer. Cell 139: 1069-1083 (2009)

52. Lindstrom S, Schumacher F R, Cox D, Travis R C, Albanes D, Allen N E, Andriole G, Berndt S I, Boeing H, Bueno-de-Mesquita H B, Crawford E D, Diver W R, Gaziano J M, Giles G G, Giovannucci E, Gonzalez C A, Henderson B, Hunter D J, Johansson M, Kolonel L N, Ma J, Le Marchand L, Pala V, Stampfer M, Stram D O, Thun M J, Tjonneland A, Trichopoulos D, Virtamo J, Weinstein S J, Willett W C, Yeager M, Hayes R B, Severi G, Haiman C A, Chanock S J, Kraft P: Common genetic variants in prostate

cancer risk prediction--results from the NCI Breast and Prostate Cancer Cohort Consortium (BPC3). Cancer Epidemiol.Biomarkers Prev. 21: 437-444 (2012)

53. Liu H, Shi J, Wilkerson M, Yang X J, Lin F: Immunohistochemical evaluation of ERG expression in various benign and malignant tissues. Ann.Clin.Lab.Sci. 43: 3-9 (2013)

54. Lokeshwar B L, Hurkadli K S, Sheth A R, Block N L: Human prostatic inhibin suppresses tumor growth and inhibits clonogenic cell survival of a model prostatic adenocarcinoma, the Dunning R3327G rat tumor. Cancer Res. 53: 4855-4859 (1993)

55. Lou H, Li H, Yeager M, Im K, Gold B, Schneider T D, Fraumeni J F,Jr, Chanock S J, Anderson S K, Dean M: Promoter variants in the MSMB gene associated with prostate cancer regulate MSMB/NCOA4 fusion transcripts. Hum.Genet. 131: 1453-1466 (2012)

56. Lou H, Yeager M, Li H, Bosquet J G, Hayes R B, Orr N, Yu K, Hutchinson A, Jacobs K B, Kraft P, Wacholder S, Chatterjee N, Feigelson H S, Thun M J, Diver W R, Albanes D, Virtamo J, Weinstein S, Ma J, Gaziano J M, Stampfer M, Schumacher F R, Giovannucci E, Cancel-Tassin G, Cussenot O, Valeri A, Andriole G L, Crawford E D, Anderson S K, Tucker M, Hoover R N, Fraumeni J F,Jr, Thomas G, Hunter D J, Dean M, Chanock S J: Fine mapping and functional analysis of a common variant in MSMB on chromosome 10q11.2 associated with prostate cancer susceptibility. Proc.Natl.Acad.Sci.U.S.A. 106: 7933-7938 (2009)

57. Luedeke M: Predisposition for *TMPRSS2-ERG* fusion in prostate cancer by variants in DNA repair genes. Rer nat Dissertation, Universität Ulm (2012)

58. MacKenzie J A, Payne R M: Mitochondrial protein import and human health and disease. Biochim.Biophys.Acta 1772: 509-523 (2007)

59. Mandair D, Rossi R E, Pericleous M, Whyand T, Caplin M E: Prostate cancer and the influence of dietary factors and supplements: a systematic review. Nutr.Metab.(Lond) 11: 30-7075-11-30. eCollection 2014 (2014)

60. Masutani M, Nakagama H, Sugimura T: Poly(ADP-ribose) and carcinogenesis. Genes Chromosomes Cancer 38: 339-348 (2003)

61. Mathis G, Althaus F R: Release of core DNA from nucleosomal core particles following (ADP-ribose)n-modification in vitro. Biochem.Biophys.Res.Commun. 143: 1049-1054 (1987)

62. Mestayer C, Blanchere M, Jaubert F, Dufour B, Mowszowicz I: Expression of androgen receptor coactivators in normal and cancer prostate tissues and cultured cell lines. Prostate 56: 192-200 (2003)

63. Meyer R G, Meyer-Ficca M L, Jacobson E L, Jacobson M K: Human poly(ADP-ribose) glycohydrolase (PARG) gene and the common promoter sequence it shares with inner mitochondrial membrane translocase 23 (TIM23). Gene 314: 181-190 (2003)

64. Mosmann T: Rapid colorimetric assay for cellular growth and survival: application to proliferation and cytotoxicity assays. J.Immunol.Methods 65: 55-63 (1983)

65. Mosquera J M, Perner S, Demichelis F, Kim R, Hofer M D, Mertz K D, Paris P L, Simko J, Collins C, Bismar T A, Chinnaiyan A M, Rubin M A: Morphological features of TMPRSS2-ERG gene fusion prostate cancer. J.Pathol. 212: 91-101 (2007)

66. Nakadate Y, Kodera Y, Kitamura Y, Tachibana T, Tamura T, Koizumi F: Silencing of poly(ADP-ribose) glycohydrolase sensitizes lung cancer cells to radiation through the abrogation of DNA damage checkpoint. Biochem.Biophys.Res.Commun. 441: 793-798 (2013)

67. Nam R K, Reeves J R, Toi A, Dulude H, Trachtenberg J, Emami M, Daigneault L, Panchal C, Sugar L, Jewett M A, Narod S A: A novel serum marker, total prostate secretory protein of 94 amino acids, improves prostate cancer detection and helps identify high grade cancers at diagnosis. J.Urol. 175: 1291-1297 (2006)

68. Ogata N, Ueda K, Hayaishi O: ADP-ribosylation of histone H2B. Identification of glutamic acid residue 2 as the modification site. J.Biol.Chem. 255: 7610-7615 (1980)

69. Ogata N, Ueda K, Kawaichi M, Hayaishi O: Poly(ADP-ribose) synthetase, a main acceptor of poly(ADP-ribose) in isolated nuclei. J.Biol.Chem. 256: 4135-4137 (1981)

70. Pathak B R, Breed A A, Nakhawa V H, Jagtap D D, Mahale S D: Growth inhibition mediated by PSP94 or CRISP-3 is prostate cancer cell line specific. Asian J.Androl. 12: 677-689 (2010)

71. Peng Y, Li C X, Chen F, Wang Z, Ligr M, Melamed J, Wei J, Gerald W, Pagano M, Garabedian M J, Lee P: Stimulation of prostate cancer cellular proliferation and invasion by the androgen receptor co-activator ARA70. Am.J.Pathol. 172: 225-235 (2008)

72. Perner S, Mosquera J M, Demichelis F, Hofer M D, Paris P L, Simko J, Collins C, Bismar T A, Chinnaiyan A M, De Marzo A M, Rubin M A: TMPRSS2-ERG fusion prostate cancer: an early molecular event associated with invasion. Am.J.Surg.Pathol. 31: 882-888 (2007)

73. Pleschke J M, Kleczkowska H E, Strohm M, Althaus F R: Poly(ADP-ribose) binds to specific domains in DNA damage checkpoint proteins. J.Biol.Chem. 275: 40974-40980 (2000)

74. Pomerantz M M, Shrestha Y, Flavin R J, Regan M M, Penney K L, Mucci L A, Stampfer M J, Hunter D J, Chanock S J, Schafer E J, Chan J A, Tabernero J, Baselga J, Richardson A L, Loda M, Oh W K, Kantoff P W, Hahn W C, Freedman M L: Analysis of the 10q11 cancer risk locus implicates MSMB and NCOA4 in human prostate tumorigenesis. PLoS Genet. 6: e1001204 (2010)

75. Powell C, Mikropoulos C, Kaye S B, Nutting C M, Bhide S A, Newbold K, Harrington K J: Pre-clinical and clinical evaluation of PARP inhibitors as tumour-specific radiosensitisers. Cancer Treat.Rev. 36: 566-575 (2010)

76. Qi M, Li Y, Liu J, Yang X, Wang L, Zhou Z, Han B: Morphologic features of carcinomas with recurrent gene fusions. Adv.Anat.Pathol. 19: 417-424 (2012)

77. Rajput A B, Miller M A, De Luca A, Boyd N, Leung S, Hurtado-Coll A, Fazli L, Jones E C, Palmer J B, Gleave M E, Cox M E, Huntsman D G: Frequency of the TMPRSS2:ERG gene fusion is increased in moderate to poorly differentiated prostate cancers. J.Clin.Pathol. 60: 1238-1243 (2007)

78. Rinckleb A E: Common germline variants for prostate cancer risk: Implication in DNA repair and *TMPRSS2-ERG* fusion formation. Hum biol Dissertation, Universität Ulm (2014)

79. Rinckleb A E, Surowy H M, Luedeke M, Varga D, Schrader M, Hoegel J, Vogel W, Maier C: The prostate cancer risk locus at 10q11 is associated with DNA repair capacity. DNA Repair (Amst) 11: 693-701 (2012)

80. Rouzier C, Haudebourg J, Carpentier X, Valerio L, Amiel J, Michiels J F, Pedeutour F: Detection of the TMPRSS2-ETS fusion gene in prostate carcinomas: retrospective analysis of 55 formalin-fixed and paraffin-embedded samples with clinical data. Cancer Genet.Cytogenet. 183: 21-27 (2008)

81. Sakai H, Tsurusaki T, Kanda S, Koji T, Xuan J W, Saito Y: Prognostic significance of beta-microseminoprotein mRNA expression in prostate cancer. Prostate 38: 278-284 (1999)

82. Shukeir N, Arakelian A, Kadhim S, Garde S, Rabbani S A: Prostate secretory protein PSP-94 decreases tumor growth and hypercalcemia of malignancy in a syngenic in vivo model of prostate cancer. Cancer Res. 63: 2072-2078 (2003)

83. Sun C, Dobi A, Mohamed A, Li H, Thangapazham R L, Furusato B, Shaheduzzaman S, Tan S H, Vaidyanathan G, Whitman E, Hawksworth D J, Chen Y, Nau M, Patel V, Vahey M, Gutkind J S, Sreenath T, Petrovics G, Sesterhenn I A, McLeod D G, Srivastava S: TMPRSS2-ERG fusion, a common genomic alteration in prostate cancer activates C-MYC and abrogates prostate epithelial differentiation. Oncogene 27: 5348-5353 (2008)

84. Sun J, Chang B L, Isaacs S D, Wiley K E, Wiklund F, Stattin P, Duggan D, Carpten J D, Trock B J, Partin A W, Walsh P C, Gronberg H, Xu J, Isaacs W B, Zheng S L: Cumulative effect of five genetic variants on prostate cancer risk in multiple study populations. Prostate 68: 1257-1262 (2008)

85. Thomas G, Jacobs K B, Yeager M, Kraft P, Wacholder S, Orr N, Yu K, Chatterjee N, Welch R, Hutchinson A, Crenshaw A, Cancel-Tassin G, Staats B J, Wang Z, Gonzalez-Bosquet J, Fang J, Deng X, Berndt S I, Calle E E, Feigelson H S, Thun M J, Rodriguez C, Albanes D, Virtamo J, Weinstein S, Schumacher F R, Giovannucci E, Willett W C,

Cussenot O, Valeri A, Andriole G L, Crawford E D, Tucker M, Gerhard D S, Fraumeni J F,Jr, Hoover R, Hayes R B, Hunter D J, Chanock S J: Multiple loci identified in a genome-wide association study of prostate cancer. Nat.Genet. 40: 310-315 (2008)

86. Ting H J, Bao B Y, Hsu C L, Lee Y F: Androgen-receptor coregulators mediate the suppressive effect of androgen signals on vitamin D receptor activity. Endocrine 26: 1-9 (2005)

87. Tomlins S A, Laxman B, Varambally S, Cao X, Yu J, Helgeson B E, Cao Q, Prensner J R, Rubin M A, Shah R B, Mehra R, Chinnaiyan A M: Role of the TMPRSS2-ERG gene fusion in prostate cancer. Neoplasia 10: 177-188 (2008)

88. Tomlins S A, Rhodes D R, Perner S, Dhanasekaran S M, Mehra R, Sun X W, Varambally S, Cao X, Tchinda J, Kuefer R, Lee C, Montie J E, Shah R B, Pienta K J, Rubin M A, Chinnaiyan A M: Recurrent fusion of TMPRSS2 and ETS transcription factor genes in prostate cancer. Science 310: 644-648 (2005)

89. Tu J J, Rohan S, Kao J, Kitabayashi N, Mathew S, Chen Y T: Gene fusions between TMPRSS2 and ETS family genes in prostate cancer: frequency and transcript variant analysis by RT-PCR and FISH on paraffin-embedded tissues. Mod.Pathol. 20: 921-928 (2007)

90. Uchiumi F, Watanabe T, Ohta R, Abe H, Tanuma S: PARP1 gene expression is downregulated by knockdown of PARG gene. Oncol.Rep. 29: 1683-1688 (2013)

91. Vander Heiden M G, Cantley L C, Thompson C B: Understanding the Warburg effect: the metabolic requirements of cell proliferation. Science 324: 1029-1033 (2009)

92. Varghese J S, Easton D F: Genome-wide association studies in common cancers--what have we learnt? Curr.Opin.Genet.Dev. 20: 201-209 (2010)

93. Wang S, Kollipara R K, Srivastava N, Li R, Ravindranathan P, Hernandez E, Freeman E, Humphries C G, Kapur P, Lotan Y, Fazli L, Gleave M E, Plymate S R, Raj G V, Hsieh J T, Kittler R: Ablation of the oncogenic transcription factor ERG by deubiquitinase inhibition in prostate cancer. Proc.Natl.Acad.Sci.U.S.A. 111: 4251-4256 (2014)

94. Warburg O: On the origin of cancer cells. Science 123: 309-314 (1956)

95. Whitaker H C, Kote-Jarai Z, Ross-Adams H, Warren A Y, Burge J, George A, Bancroft E, Jhavar S, Leongamornlert D, Tymrakiewicz M, Saunders E, Page E, Mitra A, Mitchell G, Lindeman G J, Evans D G, Blanco I, Mercer C, Rubinstein W S, Clowes V, Douglas F, Hodgson S, Walker L, Donaldson A, Izatt L, Dorkins H, Male A, Tucker K, Stapleton A, Lam J, Kirk J, Lilja H, Easton D, IMPACT Study Steering Committee, IMPACT Study Collaborators, UK GPCS Collaborators, Cooper C, Eeles R, Neal D E: The rs10993994 risk allele for prostate cancer results in clinically relevant changes in microseminoprotein-beta expression in tissue and urine. PLoS One 5: e13363 (2010)

96. Wu W, Kong Z, Duan X, Zhu H, Li S, Zeng S, Liang Y, Iliakis G, Gui Z, Yang D: Inhibition of PARP1 by small interfering RNA enhances docetaxel activity against human prostate cancer PC3 cells. Biochem.Biophys.Res.Commun. 442: 127-132 (2013)

97. Xu J, Lange E M, Lu L, Zheng S L, Wang Z, Thibodeau S N, Cannon-Albright L A, Teerlink C C, Camp N J, Johnson A M, Zuhlke K A, Stanford J L, Ostrander E A, Wiley K E, Isaacs S D, Walsh P C, Maier C, Luedeke M, Vogel W, Schleutker J, Wahlfors T, Tammela T, Schaid D, McDonnell S K, DeRycke M S, Cancel-Tassin G, Cussenot O, Wiklund F, Gronberg H, Eeles R, Easton D, Kote-Jarai Z, Whittemore A S, Hsieh C L, Giles G G, Hopper J L, Severi G, Catalona W J, Mandal D, Ledet E, Foulkes W D, Hamel N, Mahle L, Moller P, Powell I, Bailey-Wilson J E, Carpten J D, Seminara D, Cooney K A, Isaacs W B, International Consortium for Prostate Cancer Genetics: HOXB13 is a susceptibility gene for prostate cancer: results from the International Consortium for Prostate Cancer Genetics (ICPCG). Hum.Genet. 132: 5-14 (2013)

98. Yeh S, Chang C: Cloning and characterization of a specific coactivator, ARA70, for the androgen receptor in human prostate cells. Proc.Natl.Acad.Sci.U.S.A. 93: 5517-5521 (1996)

99. Yu S W, Wang H, Poitras M F, Coombs C, Bowers W J, Federoff H J, Poirier G G, Dawson T M, Dawson V L: Mediation of poly(ADP-ribose) polymerase-1-dependent cell death by apoptosis-inducing factor. Science 297: 259-263 (2002)

100. Zeltser L, Desplan C, Heintz N: Hoxb-13: a new Hox gene in a distant region of the HOXB cluster maintains colinearity. Development 122: 2475-2484 (1996)

101. Zheng S L, Sun J, Wiklund F, Smith S, Stattin P, Li G, Adami H O, Hsu F C, Zhu Y, Balter K, Kader A K, Turner A R, Liu W, Bleecker E R, Meyers D A, Duggan D, Carpten J D, Chang B L, Isaacs W B, Xu J, Gronberg H: Cumulative association of five genetic variants with prostate cancer. N.Engl.J.Med. 358: 910-919 (2008)

102. Ziegler M, Oei S L: A cellular survival switch: poly(ADP-ribosyl)ation stimulates DNA repair and silences transcription. Bioessays 23: 543-548 (2001)

Acknowledgments

The acknowledgments were removed due to data privacy.

Curriculum vitae

The curriculum vitae was removed due to data privacy.